

# 1 Increased carbon capture by a silicate-treated forested watershed 2 affected by acid deposition

3

4 Lyla L. Taylor<sup>1\*</sup>, Charles T. Driscoll<sup>2</sup>, Peter M. Groffman<sup>3</sup>, Greg H. Rau<sup>4</sup>, Joel D. Blum<sup>5</sup> and David J. Beerling<sup>1</sup>

5 <sup>1</sup>Leverhulme Centre for Climate Change Mitigation, Department of Animal and Plant Sciences, University of Sheffield,  
6 Sheffield S10 2TN, UK

7 <sup>2</sup>Department of Civil and Environmental Engineering, 151 Link Hall, Syracuse University, Syracuse, NY 13244, USA

8 <sup>3</sup>City University of New York, Advanced Science Research Center at the Graduate Center, New York, NY 10031 and Cary  
9 Institute of Ecosystem Studies, Millbrook, NY 12545 USA

10 <sup>4</sup>Institute of Marine Sciences, University of California, Santa Cruz, CA 95064 USA

11 <sup>5</sup>Department of Earth and Environmental Sciences, University of Michigan, Ann Arbor, MI 48109, USA

12 *Correspondence to:* Lyla L. Taylor (L.L.Taylor@sheffield.ac.uk)

13 **Abstract.** Meeting internationally agreed-upon climate targets requires Carbon Dioxide Removal (CDR) strategies coupled  
14 with an urgent phase-down of fossil fuel emissions. However, the efficacy and wider impacts of CDR are poorly understood.  
15 Enhanced rock weathering (ERW) is a land-based CDR strategy requiring large-scale field trials. Here we show that a low  
16 3.44 t ha<sup>-1</sup> wollastonite treatment in an 11.8-ha acid-rain-impacted forested watershed in New Hampshire, USA led to  
17 cumulative carbon capture by carbonic acid weathering of 0.025–0.13 t CO<sub>2</sub> ha<sup>-1</sup> over 15 years. Despite a 0.8–2.4 t CO<sub>2</sub> ha<sup>-1</sup>  
18 logistical carbon penalty from mining, grinding, transportation and spreading, by 2015 weathering together with increased  
19 forest productivity led to net CDR of 8.5–11.5 t CO<sub>2</sub> ha<sup>-1</sup>. Our results demonstrate that ERW may be an effective, scalable  
20 CDR strategy for acid-impacted forests but at large-scale requires sustainable sources of silicate rock dust.

## 21 1 Introduction

22 The Intergovernmental Panel on Climate Change (IPCC)(Rogelj et al., 2018) Special Report on global warming indicates  
23 large-scale deployment of Carbon Dioxide Removal (CDR) technologies will be required to avoid warming in excess of 1.5  
24 °C by the end of this century. Land-based CDR strategies include enhanced rock weathering (ERW), which aims to accelerate  
25 the natural geological process of carbon sequestration by amending soils with crushed reactive calcium (Ca) and magnesium  
26 (Mg)-bearing rocks such as basalt (The Royal Society and The Royal Academy of Engineering, 2018;Hartmann et al., 2013).  
27 Forests represent potential large-scale deployment opportunities where rock amendments may provide a range of benefits,  
28 including amelioration of soil acidification and provisioning of inorganic plant-nutrients to cation-depleted soils (Hartmann et  
29 al., 2013;Beerling et al., 2018). Although ERW has not yet been demonstrated as a CDR technique at the catchment scale, a  
30 forested watershed experiment at the Hubbard Brook Experimental Forest (HBEF, 43° 56'N, 71° 45'W) in the White

31 Mountains of New Hampshire, USA provides an unusual opportunity for assessing proof-of-concept in this priority research  
32 area.

33 The HBEF watershed experiment, designed to restore soil calcium following decades of leaching by acid rain, involved  
34 application of a finely ground rapidly-weathered calcium silicate mineral wollastonite ( $\text{CaSiO}_3$ ;  $3.44 \text{ t ha}^{-1}$ ) on 19 October  
35 1999 to an 11.8-ha forested watershed (SI Appendix) (Likens et al., 2004; Peters et al., 2004; Shao et al., 2016). Unlike the  
36 carbonate minerals (e.g.,  $\text{CaCO}_3$ ) commonly applied to acidified soils (Lundström et al., 2003), wollastonite does not release  
37  $\text{CO}_2$  when weathered (Supplementary Information) so is much better suited for CDR (Hartmann et al., 2013). It also has  
38 dissolution kinetics comparable to or faster than other calcium-rich silicate minerals such as labradorite found in basalt  
39 (Brantley et al., 2008). Thus, the HBEF experiment provides a timely and unparalleled opportunity for investigating the long-  
40 term (15 years) effects of ERW on CDR potential via forest and stream water chemistry responses.

41 In the case of ERW with wollastonite, CDR follows as Ca cations ( $\text{Ca}^{2+}$ ) liberated by weathering consume atmospheric  
42  $\text{CO}_2$  through the formation of bicarbonate ( $\text{HCO}_3^-$ ) by charge balance, as described by the following reaction:



44 However, forests in the northeastern USA have experienced acid deposition (Likens and Bailey, 2014), changes in  
45 nitrogen cycling (Goodale and Aber, 2001; McLauchlan et al., 2007) and increases in dissolved organic carbon (DOC) fluxes  
46 (Cawley et al., 2014) that may affect  $\text{CO}_2$  removal efficiency by ERW processes. In particular,  $\text{CO}_2$  consumption as measured  
47 by bicarbonate production may be diminished if sulphate ( $\text{SO}_4^{2-}$ ), nitrate ( $\text{NO}_3^-$ ), or naturally-occurring organic acid anions  
48 (Fakhraei and Driscoll, 2015) ( $\text{H}_2\text{A}^-$ ) in DOC intervene to inhibit the following mineral weathering reactions. For example:



52 These environmental effects on stream-water chemistry are well documented at the HBEF (Cawley et al., 2014; Likens and  
53 Bailey, 2014; Rosi-Marshall et al., 2016; McLauchlan et al., 2007), and may be exacerbated under future climate change  
54 (Sebestyen et al., 2009; Campbell et al., 2009).

55 Here we exploit the experimental design and long-term monitoring of streamwater chemistry, trees, and soils, for two  
56 small forested HBEF watersheds to evaluate the effects of the wollastonite treatment in 1999 on catchment  $\text{CO}_2$  consumption  
57 via inorganic and organic pathways. Further, we examine how biogeochemical perturbations in S, N, and organic carbon  
58 cycling affect catchment inorganic  $\text{CO}_2$  consumption. We consider the forest response, the carbon cost for ERW deployment  
59 (mining, grinding, transportation and application), and the net greenhouse gas balance for the treatment. Finally, we provide  
60 an initial assessment of the net CDR potential of silicate treatments deployed over larger areas of acidified forest in the  
61 northeastern United States.

62 **2 Methods**

63 This section describes the site and wollastonite treatment (Section 2.1) and our approaches for modelling the inorganic carbon  
 64 fluxes in streamwater (Section 2.2) and other greenhouse gas fluxes associated with the treatment (Section 2.3). The variables  
 65 from each of the seven equations in Methods are tabulated in Table 1 along with the section, equation, figure and table numbers  
 66 where they appear.

67

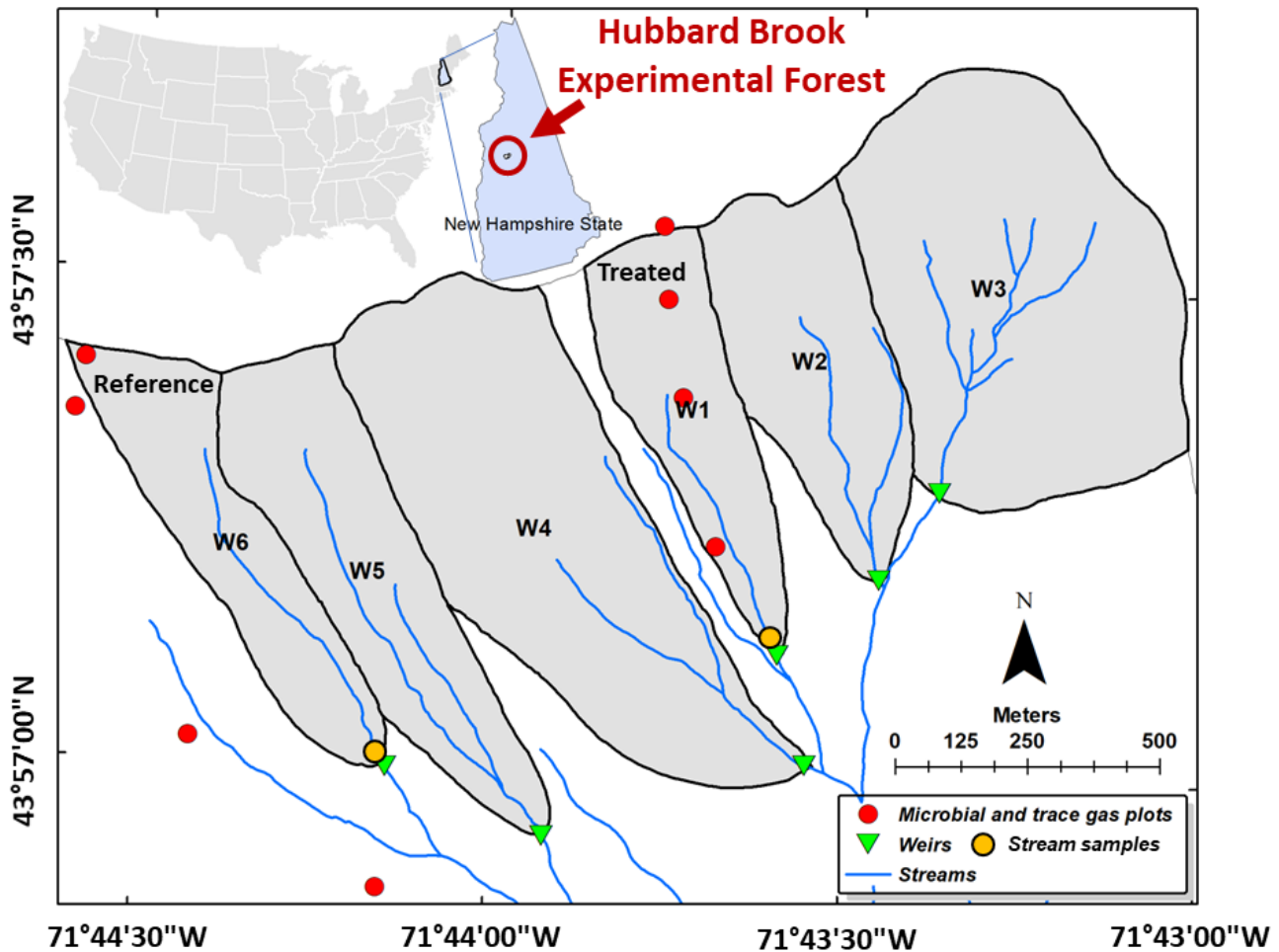
68 **Table 1. Summary of variables presented in Methods (Section 2, Eqs 1 through 7)**

Variable	Units	Sections	Equations	Figures	Tables	Description
[HCO <sub>3</sub> <sup>-</sup> ]	mol kgw <sup>-1</sup>	2.2.3, 2.2.4	1,3	2a, S5a,d,g S6a		Concentrations of solutes in water, in this case HCO <sub>3</sub> <sup>-</sup> , are denoted by square brackets.
<i>t</i>	time	2.2.3–5	1–5			Denotes individual samples in the time series
$\alpha_{\text{rain,HCO}_3}$	fraction	2.2.3, 2.2.4, Appendix A	1,2,A2	S3		Fraction of an ion, in this case HCO <sub>3</sub> <sup>-</sup> , originating from precipitation.
<i>flow</i>	mm year <sup>-1</sup>	2.2.3–5	1–5	S2d		Streamwater flow
<i>CO<sub>2</sub>,HCO<sub>3</sub></i>	mol C year <sup>-1</sup>	2.2.3, 2.2.4	1,3	2b, S5b,e,h	3,S1	Total watershed CO <sub>2</sub> consumption as calculated from bicarbonate
<i>CO<sub>2</sub>,ions</i>	mol C year <sup>-1</sup>	2.2.3	2		3	Total watershed CO <sub>2</sub> consumption as calculated from major ions
<i>Wo-CO<sub>2</sub>,HCO<sub>3</sub></i>	mol C year <sup>-1</sup>	2.2.4	3	2c,5, S5c,f,i S6b,c	3,4,S1	Watershed CO <sub>2</sub> consumption as calculated from bicarbonate resulting from wollastonite weathering. Our conservative/pessimistic <b><i>ACONS</i></b> estimate in our GHG balance is the 15-year sum.
<i>X<sub>Ca</sub></i>	fraction	2.2.3, Appendix B	3,4,B1	S1a		Fraction of total calcium originating from wollastonite
<i>Wo-CO<sub>2</sub>,Ca</i>	mol C year <sup>-1</sup>	2.2.3	4	2f, S6b,c	3, S1	Watershed CO <sub>2</sub> consumption as calculated from calcium due to wollastonite weathering. Our optimistic estimate for <b><i>ACONS</i></b> in our GHG balance is the 15-year sum.
<i>C<sub>i</sub></i>	mol kgw <sup>-1</sup>	2.2.5	5			Concentration of solute for sample <i>i</i> (collected ~monthly for chemical analysis)
<i>Q<sub>i</sub></i>	mm time <sup>-1</sup>	2.2.5	5			Streamflow for sample <i>i</i>
<i>Q<sub>k</sub></i>	mm day <sup>-1</sup>	2.2.5	5	S2b		Streamflow for day <i>k</i>
<i>N</i>	number	2.2.5	5			Number of daily flow measurements
<b><i>ΔGHG</i></b>	t CO <sub>2</sub> ha <sup>-1</sup>	2.3.1	6	5	4	Net treatment effect on watershed greenhouse gas balance
<b><i>Δwood</i></b>	t CO <sub>2</sub> ha <sup>-1</sup>	2.3.1	6	5	4	Treatment effect on woody biomass over ten years, positive if wood production increases relative to reference watershed.
<b><i>ΔCH<sub>4</sub></i></b>	t CO <sub>2</sub> ha <sup>-1</sup>	2.3.1	6	5	4	Treatment effect on soil CH <sub>4</sub> sink since 2002, positive if the soil CH <sub>4</sub> sink increases relative to reference watershed.

<b><i>ΔSRESP</i></b>	t CO <sub>2</sub> ha <sup>-1</sup>	2.3.1	6	5	4	Treatment effect on soil CO <sub>2</sub> emissions since 2002, positive if emissions decrease relative to reference watershed.
<b><i>ΔCONS</i></b>	t CO <sub>2</sub> ha <sup>-1</sup>	2.3.1	6	5	4	Treatment effect on CO <sub>2</sub> consumption over 15 years, range from <i>Wo-CO<sub>2,HCO<sub>3</sub></sub></i> and <i>Wo-CO<sub>2,Ca</sub></i>
<b><i>ΔN<sub>2</sub>O</i></b>	t CO <sub>2</sub> ha <sup>-1</sup>	2.3.1	6	5	4	Treatment effect on soil N <sub>2</sub> O emissions since 2002, positive if emissions decrease relative to reference watershed.
<b><i>ΔN<sub>03</sub>N<sub>2</sub>O</i></b>	t CO <sub>2</sub> ha <sup>-1</sup>	2.3.1	6	5	4	Treatment effect on downstream N <sub>2</sub> O emissions (due to nitrate export) over 15 years, positive if emissions decrease relative to reference watershed.
<b><i>ΔDOC</i></b>	t CO <sub>2</sub> ha <sup>-1</sup>	2.3.1	6	5	4	Treatment effect on dissolved organic carbon export over 15 years, positive if export decreases relative to reference watershed. This represents carbon loss from the watershed and likely CO <sub>2</sub> emissions downstream.
<b><i>LOGPEN</i></b>	t CO <sub>2</sub> ha <sup>-1</sup>	2.3.1	6	5	4	Logistical emissions penalty associated with mining, milling, pelletization, transport and application of the wollastonite treatment, expected to be negative.
<b><i>s</i></b>	m <sup>2</sup> kg <sup>-1</sup>	2.3.3	7			Specific surface area of material being milled
<b><i>ε<sub>p</sub></i></b>	kJ kg <sup>-1</sup>	2.3.3	7			Specific potential energy of material being milled

70 2.1 Site and treatment

71 2.1.1 Site description



72

73 **Figure 1: Location of the sampling sites and experimental watersheds.** Our streamwater samples were collected just  
74 upstream of the weirs in the treated and reference watersheds (gold disks) and our trace gas samples were collected at different  
75 elevations in treated and untreated forests (red disks).

76

77

78 The HBEF has a temperate climate with ~1400 mm mean annual precipitation of which up to one third falls as snow (Campbell  
79 et al., 2007). The mean temperatures in January and July are  $-9^{\circ}\text{C}$  and  $18^{\circ}\text{C}$  respectively, and the period from mid-May to  
80 mid-September comprises the growing season (Campbell et al., 2007). There are six small southeast-facing watersheds in the  
81 HBEF (**Fig. 1**) with 20%–30% slopes (Groffman et al., 2006), including one which received the silicate treatment (watershed

82 W1, 11.8 ha, 488–747m asl) and a biogeochemical reference (watershed W6, 13.2 ha, 545–791m asl). Carbonate and evaporite  
83 minerals are in very low abundance (<1% calcite in the crystalline rocks and glacial deposits) in these silicate-mineral  
84 dominated watersheds (Johnson et al., 1981). Well-drained Typic Haplorthod soils with pH<4.5 and mean depth 0.6m formed  
85 from relatively impermeable glacial till, which restricts water flow and protects the underlying schist bedrock from weathering.  
86 Overland runoff and flow through bedrock are both thought to be negligible (Likens, 2013). Hydrologically, the HBEF  
87 watersheds are typical of small catchments in northern New England (Sopper and Lull, 1965). Flow rates for W1 and W6  
88 along with streamwater pH are shown in Fig. S1. Prior to treatment, streamwater calcium concentrations were under 30  $\mu\text{mol}$   
89  $\text{L}^{-1}$  while bicarbonate concentrations were under 5  $\mu\text{mol L}^{-1}$ , below the ranges for typical world rivers (Moon et al., 2014) (60–  
90 2293  $\mu\text{mol Ca}^{2+} \text{L}^{-1}$ , 179–4926  $\mu\text{mol HCO}_3^- \text{L}^{-1}$ ).

91 *Fagus grandifolia*, *Betula allegheniensis* and *Acer saccharum* are the dominant trees in this Northern Hardwood forest,  
92 while *Betula papyrifera*, *Abies balsamea* and *Picea rubens* are common at the highest elevations where soils tend to be shallow  
93 and wetter (Cho et al., 2012). *A. saccharum* and *P. rubens* are both calcium-sensitive, but soil calcium-bearing minerals are  
94 less available to *A. saccharum* (Blum et al., 2002) and total bioavailable calcium content decreases with elevation (Cho et al.,  
95 2012). This silicate-addition experiment was designed to replace bioavailable calcium which had been stripped from the soils  
96 by decades of acid deposition.

### 97 2.1.2 Treatment description

98 On 19 and 21 October 1999, W1 was treated with 344  $\text{g/m}^2$  of pelletized wollastonite ( $\text{CaSiO}_3$ ) by a GPS-equipped helicopter  
99 with a motorized spreader to ensure even deployment across the catchment, including the 1804  $\text{m}^2$  streambed (Peters et al.,  
100 2004). Following treatment, the lignin-sulfonate binder forming the pellets dissolved within several days (Peters et al., 2004),  
101 and the ground wollastonite itself dissolved rapidly in the upper Oie soil horizon, increasing Oie base saturation from 40% to  
102 78% and raising soil pH from 3.88 to 4.39 within one year (Johnson et al., 2014). Although the budget of wollastonite-derived  
103 calcium (Wo-Ca) has never been closed due to lack of data from vegetation and from deeper soil layers (Shao et al., 2016), it  
104 is thought that uptake by vegetation and retention by soil exchange sites delayed transport of Wo-Ca to lower soil horizons  
105 and streamwater for three years (Johnson et al., 2014).

### 106 2.2 Geochemical modelling and $\text{CO}_2$ consumption fluxes

107  $\text{CO}_2$  consumption, the CDR pathway most closely associated with ERW, can be calculated from concentrations of either  
108 bicarbonate or the base cations released during weathering (Eq. R1). These two approaches may provide different answers if  
109 bicarbonate is reduced in the presence of other acids (Eqs. R2–R4). To calculate bicarbonate-derived  $\text{CO}_2$  consumption, we  
110 must model the speciation of dissolved inorganic carbon (DIC). This depends on two variables which must also be modelled  
111 because we do not have a time series: streamwater  $\text{pCO}_2$  and streamwater temperature. We then calculate total catchment  $\text{CO}_2$   
112 consumption fluxes and treatment effects, taking care to account for differences in sampling frequency between chemistry  
113 samples and water flow measurements.

## 114 2.2.1 Forward modelling of streamwater chemistry including dissolved inorganic carbon

115 We used a forward modelling approach to calculate dissolved streamwater bicarbonate concentrations ( $[\text{HCO}_3^-]_{\text{stream}}$ ) in the  
116 treated and reference watersheds (**Fig. 1**) over ~25 years, including 15 years post-treatment, with the United States Geological  
117 Survey (USGS) aqueous geochemistry software PHREEQC version 3.3.12-12704 (Parkhurst and Appelo, 1999) and monthly  
118 long-term (1992–2014) streamwater (Driscoll, 2016b, a) and rain/snow precipitation (Likens, 2016b, a) chemistry  
119 measurements.

120 Using MATLAB (version R2016a) scripts, we wrote PHREEQC input files and determined the inorganic carbon species  
121 for each streamwater sample with PHREEQC. Along with a standard database which decouples ammonium and nitrate  
122 (Amm.dat, provided with the PHREEQC software), we included the ionization constants for the organic acid triprotic analogue  
123 and the constants for Al complexation described for Hubbard Brook streams (Fakhraei and Driscoll, 2015) in our PHREEQC  
124 simulations. These are:  $\text{pK}_{\text{a}1}=2.02$ ,  $\text{pK}_{\text{a}2}=6.63$ ,  $\text{pK}_{\text{a}3}=7.30$ ,  $\text{pK}_{\text{Al}1}=4.07$ ,  $\text{pK}_{\text{Al}2}=7.37$ ,  $\text{pK}_{\text{Al}3}=6.65$ , and site density  $m=0.064$  mol  
125 sites  $\text{mol C}^{-1}$ . Our organic acid concentrations are the product of the corresponding site density of reactions and the measured  
126 dissolved organic carbon concentration (Fakhraei and Driscoll, 2015); these were PHREEQC inputs along with total  
127 monomeric Al and major ion concentrations from the longitudinal datasets.

128 Spectator ions ( $\text{Cl}^-$  and  $\text{NH}_4^+$ ) were adjusted to achieve charge balance given the measured pH for the treated and  
129 reference watersheds.  $\text{Cl}^-$  was only adjusted when charge balance was not achieved using  $\text{NH}_4^+$  alone. This was deemed to be  
130 the case when PHREEQC failed to converge or when the percent error exceeded 5%. We used original rather than adjusted  
131 rainwater Cl to calculate the contribution of rainwater to streamwater chemistry (described below). These adjusted ions were  
132 then held constant for our modelled scenarios, while pH was allowed to vary.

133 Exploratory PHREEQC tests (charge-balancing on DIC) either with or without organic acids suggest that the acids depress  
134 total DIC,  $\text{HCO}_3^-$  and also the saturation state of gaseous  $\text{CO}_2$ . Similar variability in the saturation is also observed when DIC  
135 values from partially degassed samples from the streams are used as input. We chose minimum and maximum values of 1100  
136 and 1700 ppm, or  $\sim 3$  and  $4.6 \times 368$ , the mean value of Mauna Loa  $\text{pCO}_2$  (Tans and Keeling, 2017) for 1985–2012. These  
137 values correspond to  $\log_{10}(\text{pCO}_2(\text{g})) = -2.87 \pm 0.09$  SD derived from a prior analysis of this variability for the same time range  
138 (Fakhraei and Driscoll, 2015).

## 139 2.2.2 Streamwater temperature

140 Air temperatures for the Hubbard Brook watersheds (Campbell, 2016) were converted to streamwater temperatures  
141 (Mohseni and Stefan, 1999). Rainwater temperatures were set equal to streamwater temperatures. These temperatures were  
142 used in our PHREEQC modelling, with equilibrium constants for the DIC species as functions of temperature. Only samples  
143 measured closest to the weirs and with a valid pH were processed with PHREEQC.

144 **2.2.3 Total catchment CO<sub>2</sub> consumption**

145 We calculate total annual watershed CO<sub>2</sub> consumption (Eq. R1) as the product of streamwater flow and streamwater  
 146 bicarbonate concentration  $[\text{HCO}_3^-]$  at time  $t$  corrected for the HCO<sub>3</sub><sup>-</sup> contribution from rainwater ( $\alpha_{\text{rain,HCO}_3}(t)$ , Appendix A):

147 
$$CO_{2,\text{HCO}_3}(t) = (1 - \alpha_{\text{rain,HCO}_3}(t)) [\text{HCO}_3^-](t) \times \text{flow}(t), \quad (1)$$

148 where  $[\text{HCO}_3^-](t)$  is given in mol kgw<sup>-1</sup> and  $\text{flow}(t)$  is the “runoff” in mm year<sup>-1</sup>. Calculated  $[\text{HCO}_3^-]$  and annual CO<sub>2</sub>  
 149 consumption for the treated and reference watersheds (Eq.1) comprise our baseline simulations and represent a primary test of  
 150 hypothesized increased carbon capture resulting from weathering of the applied silicate.

151 Bicarbonate-derived CO<sub>2</sub> consumption (Eq. 1) is the most conservative approach to estimating net carbon fluxes related  
 152 to ERW. For natural freshwaters in equilibrium with the atmosphere, this entails a titration for total alkalinity with a possible  
 153 correction for the concentration of organic acid anions (Köhler et al., 2000). However, another widely used (Jacobson and  
 154 Blum, 2003) measure of CO<sub>2</sub> consumption is derived by assuming that any base cations (Ca<sup>2+</sup>, Mg<sup>2+</sup>, K<sup>+</sup> and Na<sup>+</sup>) released  
 155 from minerals will be charge-balanced by bicarbonate formation in the oceans

156 
$$CO_{2,\text{ions}}(t) = (2[\text{Ca}^{2+}](1 - \alpha_{\text{rain,Ca}}(t)) + 2[\text{Mg}^{2+}](1 - \alpha_{\text{rain,Mg}}(t)) + [\text{K}^+](1 - \alpha_{\text{rain,K}}(t)) +$$
  
 157 
$$[\text{Na}^+](1 - \alpha_{\text{rain,Na}}(t)) - 2[\text{SO}_4^{2-}](t)) \times \text{flow}(t), \quad (2)$$

158 where the term  $-2[\text{SO}_4^{2-}](t)$  represents a commonly-applied correction for sulphuric acid weathering (Chetelat et al., 2008)  
 159 (Eq. R2). Contributions from precipitation such as  $\alpha_{\text{rain,Ca}}(t)$  are calculated by replacing bicarbonate with the individual base  
 160 cation in Eq. (A2). We tabulate  $CO_{2,\text{ions}}(t)$  results for comparison with  $CO_{2,\text{HCO}_3}(t)$  below.

161 **2.2.4 Response of CO<sub>2</sub> consumption to treatment**

162 To isolate a treatment effect for bicarbonate, we used strontium isotopes as a tracer of wollastonite (Wo) weathering within a  
 163 previously-published mixing function (Nezat et al., 2010; Peters et al., 2004) (Appendix B, **Fig. S3**). This mixing function  
 164 provides the fraction  $X_{\text{Ca}}$  of calcium originating from wollastonite (Eq. B1). We remove the contribution of all mineral sources  
 165 other than wollastonite to CO<sub>2</sub> consumption (Eq. 1), which is simulated with Ca<sup>2+</sup> concentrations reduced by  $(1 - X_{\text{Ca}})$ :

166 
$$Wo\text{-}CO_{2,\text{HCO}_3}(t) = CO_{2,\text{HCO}_3}(t) - \{[\text{HCO}_3^-](t(1 - X_{\text{Ca}}) [\text{Ca}^{2+}]) \times (1 - \alpha_{\text{rain,HCO}_3}(t)) \times \text{flow}(t)\} \quad (3)$$

167 which effectively provides a lower limit on the treatment effect.

168 We can also derive an upper limit for the treatment effect from Eq. (R1). For an ERW treatment, transient changes in  
 169 the export of ions not derived from the applied minerals may occur, but we consider that the cations released from the applied  
 170 minerals comprise the most unambiguous treatment effect in our study. The charge associated with wollastonite-derived Ca<sup>2+</sup>



171 (Wo-Ca) determines the CO<sub>2</sub> consumption associated with the HBEF wollastonite treatment. Our optimistic treatment effect  
172 based on calcium rather than bicarbonate is:

$$173 \quad Wo-CO_{2,Ca}(t) = 2 \times X_{Ca} \times [Ca^{2+}](t) \times flow(t), \quad (4)$$

174 Equations (3) and (4), together with our flux calculations accounting for sparsity of concentration data compared to daily flow  
175 data (Sec. 2.2.5), should help avoid major uncertainties in catchment-scale CO<sub>2</sub> consumption calculations: the provenance of  
176 the cations and variations in concentration and discharge (Moon et al., 2014).

### 177 2.2.5 Flux calculations

178 To ensure that fluxes from our two watersheds were comparable and to correct for the sparsity of solute measurements  
179 compared to flow measurements, we created rolling annual flow-adjusted fluxes using Method 5 of Littlewood et al. (1998) at  
180 five evenly-spaced points each year:

$$181 \quad Flux = scale \times \left[ \frac{\sum_{i=1}^M C_i Q_i}{\sum_{i=1}^M Q_i} \right] \times \left[ \frac{\sum_{k=1}^N Q_k}{N} \right], \quad (5)$$

182

183 where  $Q_i$  is the measured instantaneous stream flow,  $C_i$  is the concentration for sample  $i$ ,  $M$  is the number of streamwater  
184 chemistry samples in the year (usually 12),  $Q_k$  is the  $k^{\text{th}}$  flow measurement, and  $N$  is the number of flow measurements. In  
185 our case, daily flow measurements (Campbell, 2015) and ~monthly streamwater samples (Driscoll, 2016b, a) were available.  
186 Therefore, the mean concentration for the preceding twelve months is multiplied by the mean flow for the same period, suitably  
187 scaled to get the total annual flux. Without sub-daily timestamps for the longitudinal streamwater chemistry data, we used  
188 daily total flows rather than instantaneous flows. Tests suggested that there was little difference between using mean daily  
189 instantaneous flows and the mean daily total flows.

190

### 191 2.3 Greenhouse gas balance

192 The success of any treatment for climate change mitigation is determined by the net greenhouse gas (CO<sub>2</sub> equivalent) fluxes  
193 prior to and following treatment, at the treatment site and downstream. In addition to increased CO<sub>2</sub> consumption, desirable  
194 outcomes for a treatment include increased ecosystem carbon storage in biomass and soils, and decreases in ecosystem,  
195 downstream and logistical greenhouse gas emissions.

#### 196 2.3.1 Greenhouse gas budget for the wollastonite treatment

197 At the HBEF, we have measured the CO<sub>2</sub> consumption due to the wollastonite treatment in two different ways and these  
198 determine our range of values to be incorporated in our GHG budget. Several other treatment effects can be estimated relative  
199 to the reference watershed, but some aspects of the total GHG balance are missing. For example, we have measurements of

200 soil respiration (root+heterotrophic) and dissolved organic carbon (DOC) export in streamwater, but we lack measurements of  
201 canopy respiration from leaves and stems, and export of particulate organic carbon in streamwater. Our partial greenhouse  
202 gas budget for the HBEF wollastonite treatment will therefore be given by

203

$$204 \quad \Delta GHG = \Delta wood + \Delta SRESP + \Delta CH_4 + \Delta N_2O + \Delta CONS + \Delta NO_3N_2O + \Delta DOC + LOGPEN, \quad (6)$$

205

206 where our partial GHG treatment effect ( $\Delta GHG$ ) is the sum of greenhouse gas sink and source responses. Measured sinks for  
207 the wollastonite experiment include biomass in wood ( $\Delta wood$ ), CO<sub>2</sub> consumption ( $\Delta CONS$ ), and a soil sink for methane  
208 ( $\Delta CH_4$ ). Sources include N<sub>2</sub>O emissions both from soil ( $\Delta N_2O$ ) and exported nitrate ( $\Delta NO_3N_2O$ ), and CO<sub>2</sub> emissions from  
209 soil respiration ( $\Delta SRESP$ ), exported dissolved organic carbon ( $\Delta DOC$ ), and logistical operations ( $LOGPEN$ ).

210

211 Sink effects are defined as positive if the sink increases and are given by the difference (treated–reference) between the  
212 two watersheds, whereas source effects are defined as positive for reductions in greenhouse gas emissions (reference–treated).  
213 With these definitions, penalties are negative and reduce  $\Delta GHG$  in Eq. (6). Logistical emissions and CO<sub>2</sub> consumption due to  
214 weathering of applied wollastonite are zero for the reference watershed, so we expect  $LOGPEN$  to be negative and  $\Delta CONS$  to  
be positive.

215

216 Wood is a longer-term carbon sink than leaves or twigs so we have chosen to let this represent our biomass increment.  
217 Eq. (6) neglects ecosystem disturbances including fire, and possible carbonate mineral precipitation in soils. There is no  
evidence for the latter at the HBEF.

218

219 We used a range of emissions factors for N<sub>2</sub>O to estimate the penalty associated with nitrate export ( $\Delta NO_3N_2O$ ); low:  
0.0017 kgN<sub>2</sub>O-N kg<sup>-1</sup> DIN (Hu et al., 2016) and high: 0.0075 kgN<sub>2</sub>O-N kg<sup>-1</sup> DIN (De Klein et al., 2006), where DIN is dissolved  
220 inorganic nitrogen dominated by nitrate. This N<sub>2</sub>O was then converted to CO<sub>2e</sub> (CO<sub>2</sub> equivalents in terms of cumulative  
221 radiative forcing) given the 100-year time horizon global warming potential (Pachauri et al., 2014) (GWP<sub>100</sub>) for N<sub>2</sub>O: 265  
222 gCO<sub>2e</sub> g<sup>-1</sup> N<sub>2</sub>O. Likewise,  $\Delta CH_4$  was converted to CO<sub>2e</sub> (CO<sub>2</sub> equivalents in terms of cumulative radiative forcing) given  
223 GWP<sub>100</sub> for CH<sub>4</sub>: 28 gCO<sub>2e</sub> g<sup>-1</sup> CH<sub>4</sub>.

224

### 225 **2.3.2 Carbon sequestration in wood**

226 We calculate our treatment effect on wood production as the difference between the treated and reference watershed mean  
227 wood production (Battles et al., 2014) over two five-year periods. We considered these differences (treated–reference) to be  
228 an estimate of the treatment effect on potentially long-term (decades to centuries) biomass carbon sequestration. Assuming  
229 46.5% of the woody biomass is carbon (Martin et al., 2018), our calculated cumulative additional C sequestration in the treated  
230 watershed over ten years was 20.7 mol C m<sup>-2</sup> (9.1 t CO<sub>2</sub> ha<sup>-1</sup>). Our optimistic and pessimistic values are derived from the 95%  
231 confidence intervals for the five-year mean values (Battles et al., 2014).

### 232 2.3.3 Greenhouse gas emissions from soils

233 Measurements (Groffman, 2016) were taken at four elevations in the treated watershed and at points just west of the reference  
234 watershed starting in 2002 (Fig. 1). Gas samples were collected from chambers placed on three permanent PVC rings at each  
235 of these eight sites (Groffman, 2016). The data were not normally distributed so were analyzed with Kruskal-Wallis tests at  
236 the 0.05 significance level; however, tests with one-way ANOVA produced the same overall results. All analyses were done  
237 in Matlab R2016a.

238 Cumulative curves for each of the 24 chambers were generated by matching the dates of the measurements, excluding  
239 points which were missing data for any chamber and allowing up to a week's discrepancy between catchments. Nearly all  
240 discrepancies were within one day. Assuming diurnal variation was minor compared to seasonal variation, each datum ( $\text{g C}$   
241  $\text{m}^{-2} \text{hour}^{-1}$ ) was multiplied by 24 hours and by 30 days to get  $\text{gC m}^{-2} \text{month}^{-1}$ . There was no extrapolation to fill gaps in the  
242 dataset; results are internally consistent but not comparable to other datasets. We were particularly interested in the elevation-  
243 specific responses, as the different elevations have distinct tree species compositions and below-ground responses to the  
244 wollastonite treatment (Fahey et al., 2016).

245 The HBEF experimental watersheds are divided into  $25 \times 25\text{m}$  plots on slope-corrected grids. Vegetation has been  
246 surveyed four times since the late 1990s and assigned a zone designation in each plot (Driscoll et al., 2015; Driscoll Jr et al.,  
247 2015; Battles et al., 2015b, a) (Fig. S12). To estimate the respiration savings over the whole watershed, we added the areas of  
248 individual plots which were assigned to our four vegetation types (Low, Mid and High hardwoods, and Spruce-Fir). Because  
249 there were seven vegetation types in the datasets, we compared all types with pairwise Kruskal-Wallis tests at the 0.05  
250 significance level using the basal area data for the six dominant tree species. Kruskal-Wallis tests were appropriate because  
251 the data, and therefore the differences from the means (residuals), were not normally distributed. These tests suggested that  
252 the “extra” vegetation types (“Birch/Fern Glade”, and “Poor Hardwoods” at High and Mid elevations) could be combined with  
253 Spruce-Fir, High and Mid Hardwoods respectively. Watershed fractions for our combined forest types were 0.155 for  
254 SpruceFir, 0.16 for High Hardwoods, 0.415 for Mid Hardwoods, and 0.27 for Low Hardwoods. When creating our composite  
255 treatment effects for the entire watershed, we considered a treatment effect to be present only where our statistical analyses  
256 suggested significantly different fluxes.

### 257 2.3.4 Logistical carbon emissions costs

258 We used the 1999 upstate New York  $\text{CO}_2$  emission factor for electricity generation from oil (United States Environmental  
259 Protection Agency, 1999) ( $0.9 \text{ Mg CO}_2 \text{ MWh}^{-1}$ ), and rearranged Equation 28 of Stamboliadis (Stamboliadis et al., 2009):

$$260 \quad e_p = \frac{\left[ e^{\frac{(\ln^2/\alpha)}{\mu}} \right]}{3600 \times 1000}, \quad (7)$$

261 where the specific surface area  $s$  ( $1600 \text{ m}^2 \text{ kg}^{-1}$  for our treatment) is related to the specific potential energy  $e_p$  of the material  
262 ( $\text{kJ kg}^{-1}$ ), with theoretical parameters (Stamboliadis et al., 2009)  $\alpha=139 \text{ m}^2 \text{ kJ}^{-1}$  and  $\mu=0.469$  (dimensionless). We convert this

263 potential energy to  $\text{MWh t}^{-1} \text{Qz}$  (3600 seconds per hour and  $1000 \text{ kWh MWh}^{-1}$ ). The equation was derived for quartz (Qz)  
264 which has hardness 7. Because wollastonite hardness is in the range 5–5.5, this equation may overestimate the energy needed  
265 to grind the wollastonite.

266 The main energy source in Allerton will have been coal, and the 1999 Illinois emissions factor (United States  
267 Environmental Protection Agency, 1999) is  $1.1 \text{ Mg CO}_2 \text{ MWh}^{-1}$ . The monetary cost is  $\text{USD}0.041 \text{ kWh}^{-1}$  for pelletization of  
268 limestone fines and  $\text{USD}0.85 \text{ t}^{-1}$  product, so we estimate  $20.73 \text{ kWh t}^{-1}$  product.

269 Road transport distances were estimated using Google Maps (1397 km Gouverneur to Allerton, 1757 km Allerton to  
270 Woodstock, 408 km Gouverneur to Woodstock). We used standard emissions ranges (Sims et al., 2014) for Heavy Duty  
271 Vehicles (HDVs) ( $70\text{--}190 \text{ gCO}_2 \text{ km}^{-1} \text{ t rock}^{-1}$ ) and for short-haul cargo aircraft ( $1200\text{--}2900 \text{ gCO}_2 \text{ km}^{-1} \text{ t}^{-1}$ ). Calculation details  
272 are given in Table 2. The Matlab script used for these calculations is available on request. Note: t refers to megagrams, not US  
273 short tons.

274

275

277 **Table 2.** Logistical penalty calculations for the Hubbard Brook wollastonite treatment

<b>Penalty element</b>	<b>Value and calculation with units</b>
Mass of wollastonite (CaSiO <sub>3</sub> ) shipped to Allerton (t <sup>a</sup> Wo)	109665 lbs or <b>49.7432073 t Wo</b>
Mass of pellets shipped from Allerton (t pellets)	112992 lbs or <b>51.2523091 t pellets</b>
Ratio of pellet mass to Wollastonite mass	<b>1.0368</b> = 51.25 t pellets / 49.74 t Wo
HDV transport distance (km)	<b>3154 km</b> = 1397 km (Gouverneur to Allerton) + 1757 km (Allerton to Woodstock)
Transport distance for “local pelletization” calculation (km)	<b>408 km</b> (Gouverneur to Woodstock)
Optimistic transport emissions (g CO <sub>2</sub> g <sup>-1</sup> Wo applied)	<b>0.229 g CO<sub>2</sub> g<sup>-1</sup> Wo applied</b> = 70 gCO <sub>2</sub> km <sup>-1</sup> shipped t <sup>-1</sup> shipped × ((1397 km × 49.74 t Wo shipped) + (1757 km × 51.25 t pellets shipped)) / 48.86 × 10 <sup>6</sup> g Wo applied
Pessimistic transport emissions (g CO <sub>2</sub> g <sup>-1</sup> Wo applied)	<b>0.620 g CO<sub>2</sub> g<sup>-1</sup> Wo applied</b> = 190 gCO <sub>2</sub> km <sup>-1</sup> shipped t <sup>-1</sup> shipped × ((1397 km × 49.74 t Wo shipped) + (1757 km × 51.25 t pellets shipped)) / 48.86 × 10 <sup>6</sup> g Wo applied
Mass of pellets deployed by helicopter (t pellets applied)	110992 lbs or <b>50.3451243 t pellets applied</b>
Mass of wollastonite deployed by helicopter (t Wo applied)	<b>48.86 t Wo applied</b> = 50.345 t pellets applied / 1.03684
Total area treated (ha)	<b>14.2 ha</b> = 11.8 ha watershed plus 2.4 ha “destructive area” along the western edge
Nominal mean round trip flight distance (km, Woodstock to watershed and back)	<b>5 km</b>
Number of flights (1 short ton hopper capacity) <sup>b</sup>	<b>55.5</b> = 50.345 t pellets / 0.907 t per trip
Molar mass of wollastonite CaSiO <sub>3</sub> (g Wo mol <sup>-1</sup> Wo)	<b>116.17 g Wo mol<sup>-1</sup> Wo</b> = 40.08 g Ca mol <sup>-1</sup> Ca + 28.09 g Si mol <sup>-1</sup> Si + 3 × 16 g O mol <sup>-1</sup> O
Molar mass of CO <sub>2</sub> (g CO <sub>2</sub> mol <sup>-1</sup> CO <sub>2</sub> )	<b>44.01 g CO<sub>2</sub> mol<sup>-1</sup> CO<sub>2</sub></b> = 2 × 16 g O mol <sup>-1</sup> O + 12.01 g C mol <sup>-1</sup> C
Optimistic spreading emissions (mol CO <sub>2</sub> ha <sup>-1</sup> )	<b>483.36 mol CO<sub>2</sub> ha<sup>-1</sup></b> = 1200 gCO <sub>2</sub> km <sup>-1</sup> t <sup>-1</sup> × 5 km × 50.345 t pellets / 44.01 g CO <sub>2</sub> mol <sup>-1</sup> CO <sub>2</sub> / 14.2 ha
Optimistic spreading emissions (g CO <sub>2</sub> g <sup>-1</sup> Wo)	<b>0.006 g CO<sub>2</sub> g<sup>-1</sup> Wo</b> = 1200 gCO <sub>2</sub> km <sup>-1</sup> t <sup>-1</sup> × 5 km × 50.345 t pellets / 48.86 / 10 <sup>6</sup> g Wo
Pessimistic spreading emissions (mol CO <sub>2</sub> ha <sup>-1</sup> )	<b>1168.1 mol CO<sub>2</sub> ha<sup>-1</sup></b> = 2900 gCO <sub>2</sub> km <sup>-1</sup> t <sup>-1</sup> × 5 km × 50.345 t pellets / 44.01 g CO <sub>2</sub> mol <sup>-1</sup> CO <sub>2</sub> / 14.2 ha
Pessimistic spreading emissions (g CO <sub>2</sub> g <sup>-1</sup> Wo)	<b>0.015 g CO<sub>2</sub> g<sup>-1</sup> Wo applied</b> = 2900 gCO <sub>2</sub> km <sup>-1</sup> t <sup>-1</sup> × 5 km × 50.345 t pellets / 48.86 × 10 <sup>6</sup> g Wo applied

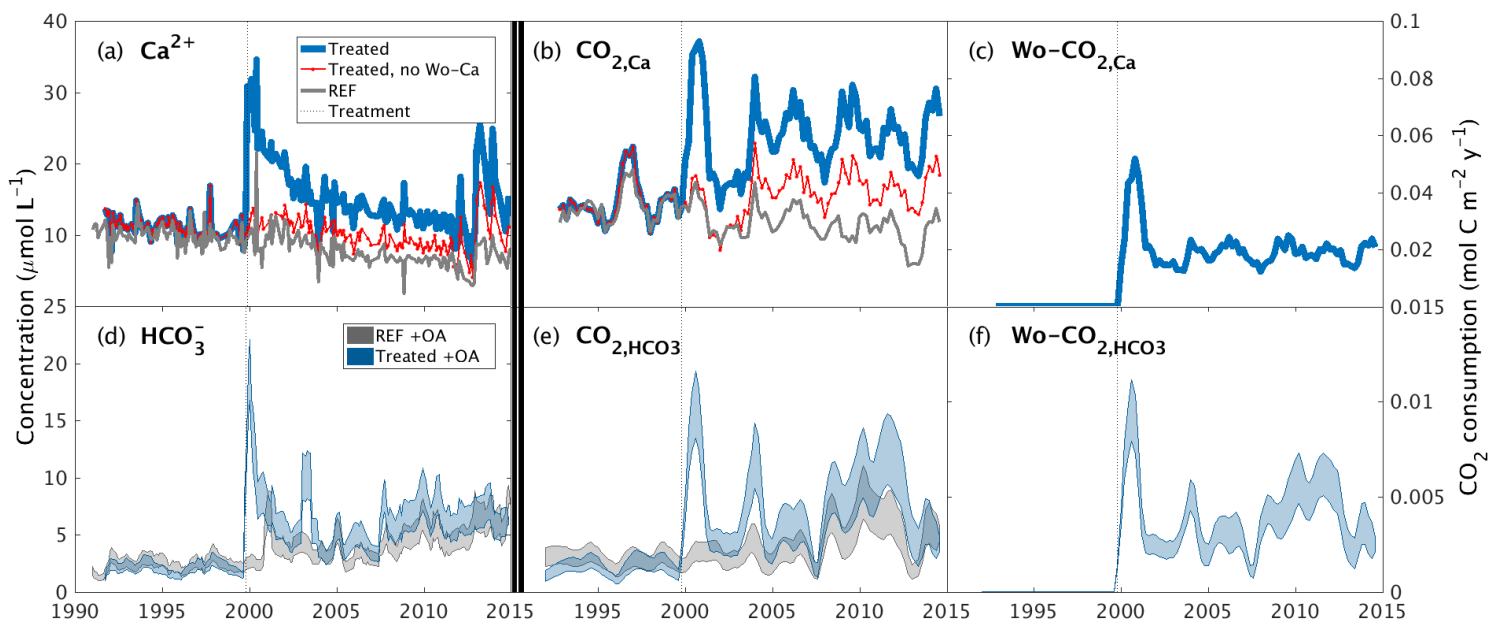
278

279 <sup>a</sup>Megagrams or metric tons, not short tons

280 <sup>b</sup>Number of flights does not explicitly enter into penalty calculations because the emissions for shorthaul aircraft are multiplied  
 281 by the 5km round trip distance and the entire mass transported, rather than the mass transported during one round trip (one  
 282 short ton).

283

284



288 **Figure 2: Inorganic CO<sub>2</sub> capture at the Hubbard Brook Experimental Forest.** (a) Observed calcium and (b) calcium export in the  
 289 reference (grey) and treated (blue) watersheds along with the contribution from sources other than wollastonite (red) and the time of treatment  
 290 (vertical dotted line). (c) Calculated CO<sub>2</sub> consumption due to the treatment ( $Wo-CO_{2,Ca}$ , Eq. 9). (d) Modelled streamwater bicarbonate, (e)  
 291 CO<sub>2</sub> consumption ( $CO_{2,HCO_3}$ , Eq. 5), and (f) CO<sub>2</sub> consumption due to the treatment ( $Wo-CO_{2,HCO_3}$ , Eq. 7), colours as for calcium. Simulations  
 292 (d–f) account for the presence of organic acids (+OA). All calcium export (b) and CO<sub>2</sub> consumption curves (c,e,f) were calculated with  
 293 flow-normalised concentrations and corrected for sparsity of samples (Methods).

294

295 We first consider the time-series of streamwater changes in Ca<sup>2+</sup> concentrations in the treated ( $[Ca]_{Treated}$ ) and reference  
 296 ( $[Ca]_{Ref}$ ) watersheds. Immediately after treatment,  $[Ca]_{Treated}$  increased from  $<30 \mu\text{mol L}^{-1}$  to  $\sim 60 \mu\text{mol L}^{-1}$ , and then slowly  
 297 declined over the next decade, remaining persistently above  $[Ca]_{Ref}$  for 15 years (**Fig. 2a**). The initial post-treatment peak  
 298 represents dissolution of wollastonite within the stream (Peters et al., 2004) and release of calcium from hyporheic exchange  
 299 during the first few years (Shao et al., 2016; Nezat et al., 2010). Retention of Ca<sup>2+</sup> ions liberated by wollastonite dissolution  
 300 (Wo-Ca) in the watershed soils (Nezat et al., 2010) and sequestration into tree biomass (Balogh-Brunstad et al., 2008; Nezat et  
 301 al., 2010) delayed appearance in streamwater for three years (Shao et al., 2016; Nezat et al., 2010). Subsequently,  $[Ca]_{Treated}$   
 302 remained approximately double  $[Ca]_{Ref}$ , with a  $\sim 30\%$  contribution from non-wollastonite Ca<sup>2+</sup> until 2012. Towards the end of  
 303 the time-series, increased seasonal NO<sub>3</sub><sup>-</sup> export in the treated watershed between 2012 and 2014 (Rosi-Marshall et al., 2016)  
 304 led to Wo-Ca displacing non-Wo-Ca from the soil exchanger.

305 We derived the annual export of  $\text{Ca}^{2+}$  from the treated and reference watersheds as the product of mean annual flow-  
306 adjusted  $\text{Ca}^{2+}$  streamwater concentrations and annual flow (**Fig. 2b**) (Methods). After accounting for variations in flow,  
307 increased streamwater  $\text{Ca}^{2+}$  concentrations in the treated watershed are translated into a 2-fold increase in total  $\text{Ca}^{2+}$  export  
308 relative to the reference watershed that was maintained for 15 years until 2015 through this analysis period. Overall, the  
309 wollastonite treatment resulted in a sharp spike in calculated  $\text{CO}_2$  consumption ( $Wo\text{-CO}_{2,\text{Ca}}$ ) that decreased but remained  
310 elevated as a result of the treatment (**Fig. 2c**).

311 Temporal patterns in modelled streamwater bicarbonate concentration in both treated and reference watersheds (**Fig.**  
312 **2d**), and the corresponding total annual  $\text{CO}_2$  consumption ( $\text{CO}_{2,\text{HCO}_3}$ ) (**Fig. 2e**) and  $\text{CO}_2$  consumption resulting from treatment  
313 ( $Wo\text{-CO}_{2,\text{HCO}_3}$ ) (**Fig. 2f**), largely mirror changes in streamwater  $\text{Ca}^{2+}$  concentrations but are modified by the supply and loss of  
314 anions. Calculated flow-adjusted  $\text{CO}_2$  consumption (**Fig. 2e**) peaked 2–3 years post-treatment with a broader peak in  $\text{CO}_2$   
315 consumption evident in 2007–2012 corresponding to declining legacy effects of acid rain until transient  $\text{NO}_3^-$  peaks appeared  
316 2012–2015.  $Wo\text{-CO}_{2,\text{HCO}_3}$  shows a pattern that mirrors  $Wo\text{-CO}_{2,\text{Ca}}$  but is generally 5 times lower (**Fig. 2c,f**).

### 317 **3.2 Sulphuric, nitric and organic acids reduce CDR**

318 We next undertook sensitivity analyses to investigate the effects of acid deposition, increased  $\text{NO}_3^-$  and organic acid export  
319 from the treated watershed on bicarbonate concentrations and resulting  $\text{CO}_2$  consumption (**Fig. S5**). In a ‘Low  $\text{SO}_4$ ’ scenario  
320 (**Fig. S5a–c**), we sought to understand the effects of acid deposition by replacing the mean monthly time-series of streamwater  
321 and rainwater  $\text{SO}_4^{2-}$  for the treated watershed with a new time-series (purple curve, **Fig. S5a**) created by repeating the post-  
322 2010 datasets, which reflect diminished acid deposition following emission controls from the US Clean Air Act (Likens and  
323 Bailey, 2014). Removing acid rain effects in this manner dramatically increased the calculated bicarbonate concentrations and  
324 total annual  $\text{CO}_2$  consumption ( $\text{CO}_{2,\text{HCO}_3}$ ), increasing the initial spikes resulting from the wollastonite treatment in both by at  
325 least four-fold (purple curves, **Fig. S5 b,c**). An additional legacy of acidification in North American forests (Harrison et al.,  
326 1989) is  $\text{SO}_4^{2-}$  retention on soil clay mineral Fe and Al oxides (Fuller et al., 1987), which were subsequently released by  
327 increased soil pH following wollastonite weathering (Shao et al., 2016;Fakhraei et al., 2016). To assess the effect of this  
328 legacy  $\text{SO}_4^{2-}$ , we ran simulations for the treated watershed substituting the lower streamwater  $\text{SO}_4^{2-}$  concentrations from the  
329 reference watershed (T REF, green curves, **Fig. S5b,c**). Results suggest that legacy  $\text{SO}_4^{2-}$  accounts for over half of the total  
330 acid deposition effect on increased  $[\text{HCO}_3^-]$  and  $\text{CO}_2$  consumption in the simulations.

331 In the ‘Ref  $\text{NO}_3$ ’ scenario (**Fig. S5 d–f**), seasonal spikes in streamwater export of  $\text{NO}_3^-$  recorded from the treated  
332 watershed between 2012 and 2015 were removed by substituting the reference watershed streamwater  $\text{NO}_3^-$  concentration  
333 measurements lacking these spikes. This manipulation markedly increased modelled bicarbonate (**Fig. S5e**) and mean annual  
334  $\text{CO}_2$  consumption (**Fig. S5f**). To quantify the effects of organic acids on bicarbonate production in the treated watershed, we  
335 ran “+OA” and “-OA” simulations, i.e., with and without accounting for organic acids, respectively (**Fig. S5 g–i**). Results  
336 showed that removing OA from our simulations also increased modelled streamwater bicarbonate concentration (**Fig. S5h**),  
337 and resulting  $\text{CO}_2$  consumption (**Fig. S5i**), in the treated watershed.

### 338 3.3 Effects of increasing wollastonite treatment

339 Because the HBEF application rate (3.44 t ha<sup>-1</sup>) is smaller than the 10–50 t ha<sup>-1</sup> suggested for ERW strategies (Strefler et al.,  
 340 2018; Beerling et al., 2018), we simulated the possible effects of a ten-fold increase in the streamwater Ca<sup>2+</sup> concentrations on  
 341 bicarbonate production (Fig. S6a) and CO<sub>2</sub> consumption (Fig. S6b). In this initial assessment, we assume streamwater  
 342 responses are directly proportional to wollastonite application rate, i.e., 34.4 t ha<sup>-1</sup>, and that all other variables remained  
 343 unchanged. Results show that after 15 years, cumulative *Wo-CO<sub>2,HCO<sub>3</sub></sub>* is 73% of *Wo-CO<sub>2,Ca</sub>* (Fig. S6c), as opposed to less than  
 344 20% for the actual rate of 3.44 t ha<sup>-1</sup> (Table 3). These results suggest that at higher application rates of wollastonite, the details  
 345 of the CO<sub>2</sub> consumption calculations become less important.

346

347 **Table 3.** Cumulative fluxes from treatment date calculated with streamwater partial pressure of CO<sub>2</sub> (gas) = 3.63 × atmospheric  
 348 CO<sub>2</sub> partial pressure measured at Mauna Loa (Tans and Keeling, 2017) (see Methods). DIC = dissolved inorganic carbon.  
 349 Scenarios are defined in the main text.

Cumulative fluxes 1 year post-treatment date (19 October 2000)								
Watershed	Scenario	Org. acids	<i>CO<sub>2,ions</sub></i>	<i>Wo-CO<sub>2,Ca</sub></i>	DIC	HCO <sub>3</sub>	<i>CO<sub>2,HCO<sub>3</sub></sub></i>	<i>Wo-CO<sub>2,HCO<sub>3</sub></sub></i>
			(Eq. 2)	(Eq. 4)			(Eq. 1)	(Eq. 3)
mol C m <sup>-2</sup>								
REF (6)	baseline	+OA	-0.003	0	0.084	0.002	0.002	0
Treated (1)	baseline	+OA	0.047	0.052	0.086	0.011	0.011	0.011
Treated (1)	baseline	-OA	0.047	0.052	0.094	0.019	0.019	0.018
Treated (1)	Low SO4	+OA	0.083	0.052	0.117	0.043	0.042	0.039
Treated (1)	REF NO3	+OA	0.047	0.052	0.105	0.030	0.030	0.029
Treated (1)	WoX10	+OA	0.513	0.534	0.533	0.457	0.457	0.457
Cumulative fluxes 15 years post-treatment (20 November 2014)								
Watershed	Scenario	Org. acids	<i>CO<sub>2,ions</sub></i>	<i>Wo-CO<sub>2,Ca</sub></i>	DIC	HCO <sub>3</sub>	<i>CO<sub>2,HCO<sub>3</sub></sub></i>	<i>Wo-CO<sub>2,HCO<sub>3</sub></sub></i>
			(Eq. 2)	(Eq. 4)			(Eq. 1)	(Eq. 3)
mol C m <sup>-2</sup>								
REF (6)	baseline	+OA	-0.274	0	1.307	0.052	0.036	0
Treated (1)	baseline	+OA	-0.044	0.294	1.299	0.083	0.064	0.057
Treated (1)	baseline	-OA	-0.044	0.294	1.414	0.198	0.179	0.145
Treated (1)	Low SO4	+OA	0.269	0.294	1.523	0.307	0.270	0.179
Treated (1)	REF NO3	+OA	-0.044	0.294	1.410	0.194	0.175	0.127
Treated (1)	WoX10	+OA	2.600	3.275	3.626	2.406	2.387	2.380

350

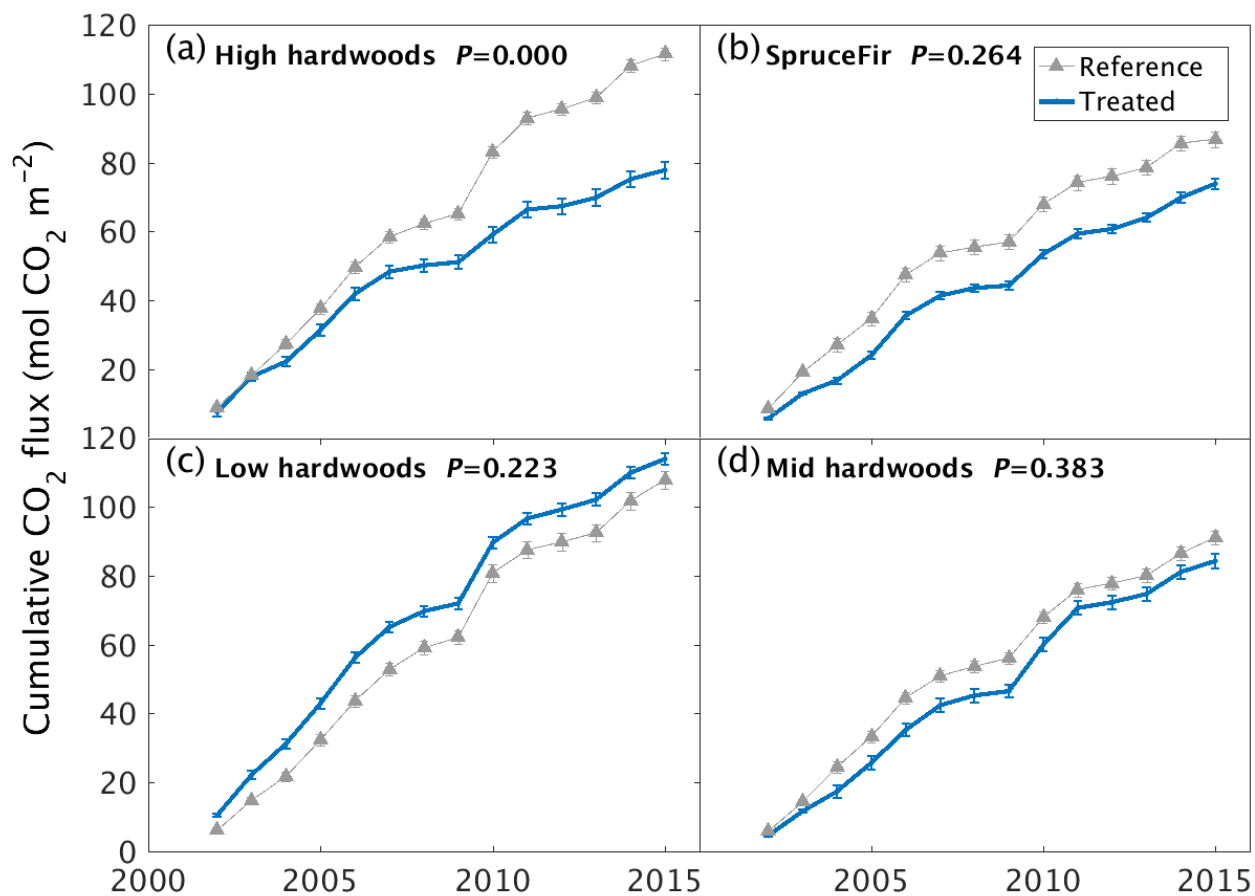


351  
352  
353  
354

### 355 **3.4 Amplification of organic carbon sequestration by wollastonite treatment**

356 In reversing long-term  $\text{Ca}^{2+}$  depletion of soils, the silicate rock treatment significantly increased forest growth and wood  
357 production between 2–12 years post-treatment relative to the reference watershed (Battles et al., 2014). This forest response  
358 increased total carbon sequestration by 20.7 mol C  $\text{m}^{-2}$  or 9.1 t  $\text{CO}_2$   $\text{ha}^{-1}$  during those ten years as a result of the treatment  
359 (Methods).

360 Changes in greenhouse gas (GHG) emissions from soils represent a further route to affecting the climate mitigation  
361 potential of the wollastonite treatment. Despite a rapid increase of one pH unit in the upper organic soil horizon (Oie), soil  
362 respiration  $\text{CO}_2$  fluxes showed no significant difference between watersheds during the first three years after treatment  
363 (Groffman et al., 2006). However, our analysis of newly available longer-term datasets indicates that the treatment  
364 significantly reduced soil respiration in the high elevation hardwood zone (~660–845m a.s.l.) ( $\chi^2(1,270)=17.2$ ,  $P < 0.001$ ),  
365 possibly due to reduced fine-root biomass (Fahey et al., 2016) rather than changes in microbial activity (Groffman et al., 2006).  
366 No significant effects on soil respiration were detected in any of the other HBEF vegetation zones (**Fig. 3**). The wollastonite  
367 treatment increased the soil sink strength for  $\text{CH}_4$  ( $\chi^2(1,266)=30.8$ ,  $P < 0.001$ ) in the low-elevation hardwood zone (482–565m  
368 a.s.l.), while it decreased in the high elevation zone ( $\chi^2(1,268)=22.3$ ,  $P < 0.001$ ) (SI Appendix, Fig. S8). There were no  
369 significant treatment effects on soil  $\text{N}_2\text{O}$  fluxes in any vegetation zone (SI Appendix).



370

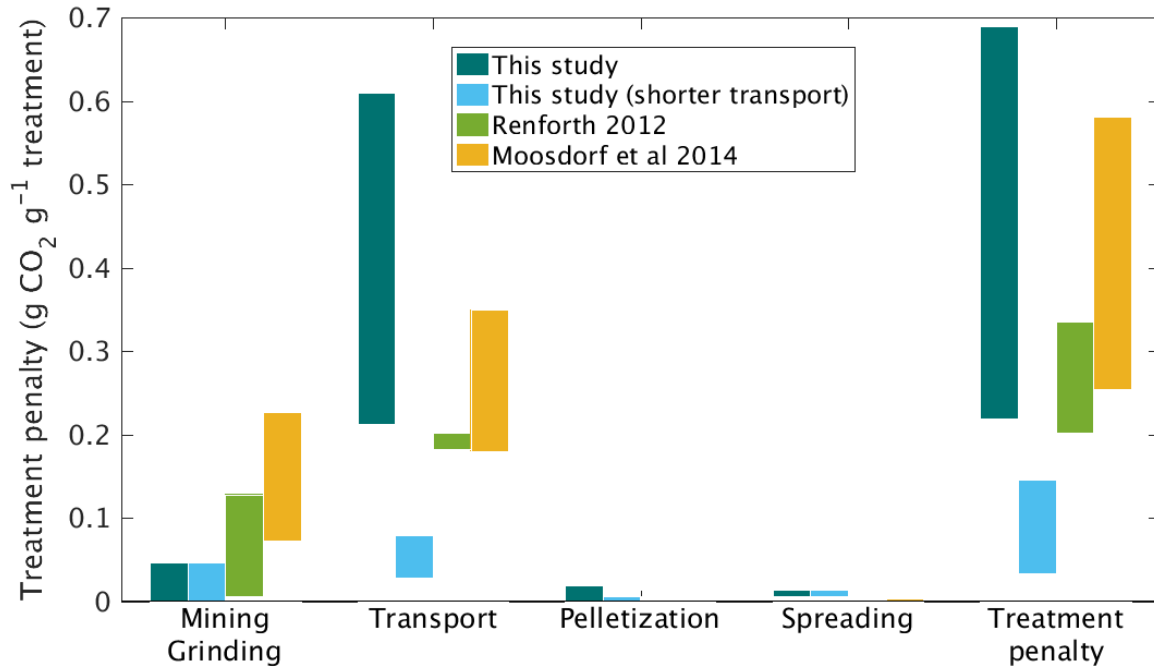
371 **Figure 3: Long-term soil respiration responses to wollastonite treatment at Hubbard Brook Experimental Forest.** Cumulative soil  
 372 CO<sub>2</sub> respiration responses of treated and untreated (a) high elevation hardwoods, (b) high elevation conifers, (c) low elevation hardwoods or  
 373 (d) mid-elevation hardwoods. Plots show cumulative means ± 1 SE for three chamber measurements at each site and time. Reference data  
 374 were collected from untreated forests immediately adjacent to the western edge of our reference catchment. P-values from Kruskal-Wallis  
 375 tests comparing treated and reference raw data (SI Appendix) are shown.

376

### 377 3.5 Logistical CO<sub>2</sub> emissions and net CDR

378 We next considered carbon emissions (penalties) for logistical operations involved in mining, grinding, transporting and  
 379 applying the wollastonite (Fig. 4, Table 2). In the HBEF experiment, wollastonite was mined and milled on site near  
 380 Gouverneur, New York. We used CO<sub>2</sub> emissions factors for electricity generation in upstate New York (United States  
 381 Environmental Protection Agency, 1999) to estimate the maximum CO<sub>2</sub> penalty for mining and grinding to the mean particle

382 size 16  $\mu\text{m}$  diameter (Methods). However, local hydropower (Energy Information Administration, 1997) and regional nuclear  
 383 power suggest these costs could have been zero. This would represent a substantial carbon saving for the overall ERW process  
 384 relative to prior expectation of ERW studies in which grinding  $\text{CO}_2$  emissions account for up to 30% reduction in ERW-CDR  
 385 efficiency (Renforth, 2012; Moosdorf et al., 2014).



386

387 **Figure 4: Carbon penalties for the wollastonite treatment.** Carbon penalties for logistic elements of the treatment are compared with  
 388 literature estimates for large-scale rollout of enhanced rock weathering for the HBEF treatment ( $3.44 \text{ t ha}^{-1}$ ), with and without long-distance  
 389 transport for pelletization.

390

391 In the HBEF experiment, the milled wollastonite was transported by highway to Allerton, Illinois, for pelletization  
 392 and then returned to the staging area near Woodstock, New Hampshire (round trip  $>3150 \text{ km}$ ). Transportation  $\text{CO}_2$  emissions  
 393 were  $0.22\text{--}0.61 \text{ t CO}_2 \text{ t Wo}^{-1}$ . Given coal power in central Illinois, we estimate pelletization emitted up to  $0.02 \text{ t CO}_2 \text{ t Wo}^{-1}$   
 394 (Methods). Application at Hubbard Brook occurred via 55  $\sim 5\text{-km}$  helicopter flights, which gives a further  $\text{CO}_2$  cost of  $0.01\text{--}$   
 395  $0.15 \text{ t CO}_2 \text{ t Wo}^{-1}$ . In total, these logistical operations emitted  $0.23\text{--}0.69 \text{ t CO}_2 \text{ t Wo}^{-1}$ , or  $0.8\text{--}2.4 \text{ t CO}_2 \text{ ha}^{-1}$  for the  $11.8 \text{ ha}$  of  
 396 the HBEF treated watershed (**Table 4**). However, local pelletization could have reduced heavy duty vehicle (HDV) transport  
 397 distance to  $\sim 400 \text{ km}$  and lowered total  $\text{CO}_2$  emitted during logistical operations to  $0.04\text{--}0.15 \text{ t CO}_2 \text{ t Wo}^{-1}$ . At other forested  
 398 sites, where wind-drift of material is not critical, pelletization may not be necessary.

399

400 **Table 4.** Measured elements of the treatment effect on the greenhouse gas budget for the Hubbard Brook Experimental Forest  
 401 wollastonite experiment.

Equation 14	Greenhouse gas sinks <sup>a</sup> and emissions <sup>a</sup> (t CO <sub>2e</sub> ha <sup>-2</sup> )	Pessimistic	Optimistic
<b>Ecosystem responses<sup>b</sup></b>			
<i>Δwood</i>	Wood production sink increased over ten years <sup>c</sup>	8.946	9.542
<i>ΔSRESP</i>	Soil respiratory CO <sub>2</sub> emissions have reduced <sup>a</sup> since 2002	2.213	2.646
<i>ΔCH<sub>4</sub></i>	Soil methane sink has increased since 2002	0.015	0.029
<i>ΔN<sub>2</sub>O</i>	Soil N <sub>2</sub> O emissions since 2002 (no significant difference)	0	0
	<b>Net ecosystem response at the treatment site through 2014</b>	<b>11.174</b>	<b>12.218</b>
<b>Downstream sequestration and emissions responses</b>			
<i>ΔCONS</i>	CO <sub>2</sub> consumption sink through 2014 ( <i>Wo-CO<sub>2,HCO<sub>3</sub></sub></i> and <i>Wo-CO<sub>2,Ca</sub></i> )	0.025	0.129
<i>ΔNO<sub>3</sub>N<sub>2</sub>O</i>	Downstream N <sub>2</sub> O emissions <sup>d</sup> from treatment date through 2014	-0.071	-0.016
<i>ΔDOC</i>	DOC export emissions <sup>d,e</sup> from treatment date through 2014	-0.203	0
	<b>Net downstream balance through 2014</b>	<b>-0.228</b>	<b>-0.129</b>
<b>Logistics:</b>			
	Mining/Grinding given hydro or nuclear/petroleum power	-0.162	0
	Helicopter (~55 5-km flights)	-0.051	-0.021
	HDV transport (New York to Illinois to New Hampshire)	-2.135	-0.787
	Pelletization (in Illinois, coal power)	-0.068	0
<i>LOGPEN</i>	<b>Total logistical emissions</b>	<b>-2.416</b>	<b>-0.808</b>
<i>ΔGHG</i>	<b>Partial treatment effect on greenhouse gas balance</b>	<b>8.509</b>	<b>11.523</b>

402 <sup>a</sup>Defined as the difference between watersheds: treated–reference for sinks and reference–treated for emissions

403 <sup>b</sup>Some possible treatment responses such as canopy respiration and particulate organic carbon export are unknown.

404 <sup>c</sup>After Battles et al. (2014). We have not attempted to extrapolate these results.

405 <sup>d</sup>ΔDOC and ΔNO<sub>3</sub>N<sub>2</sub>O are penalties because these lead to CO<sub>2</sub> and N<sub>2</sub>O emissions downstream.

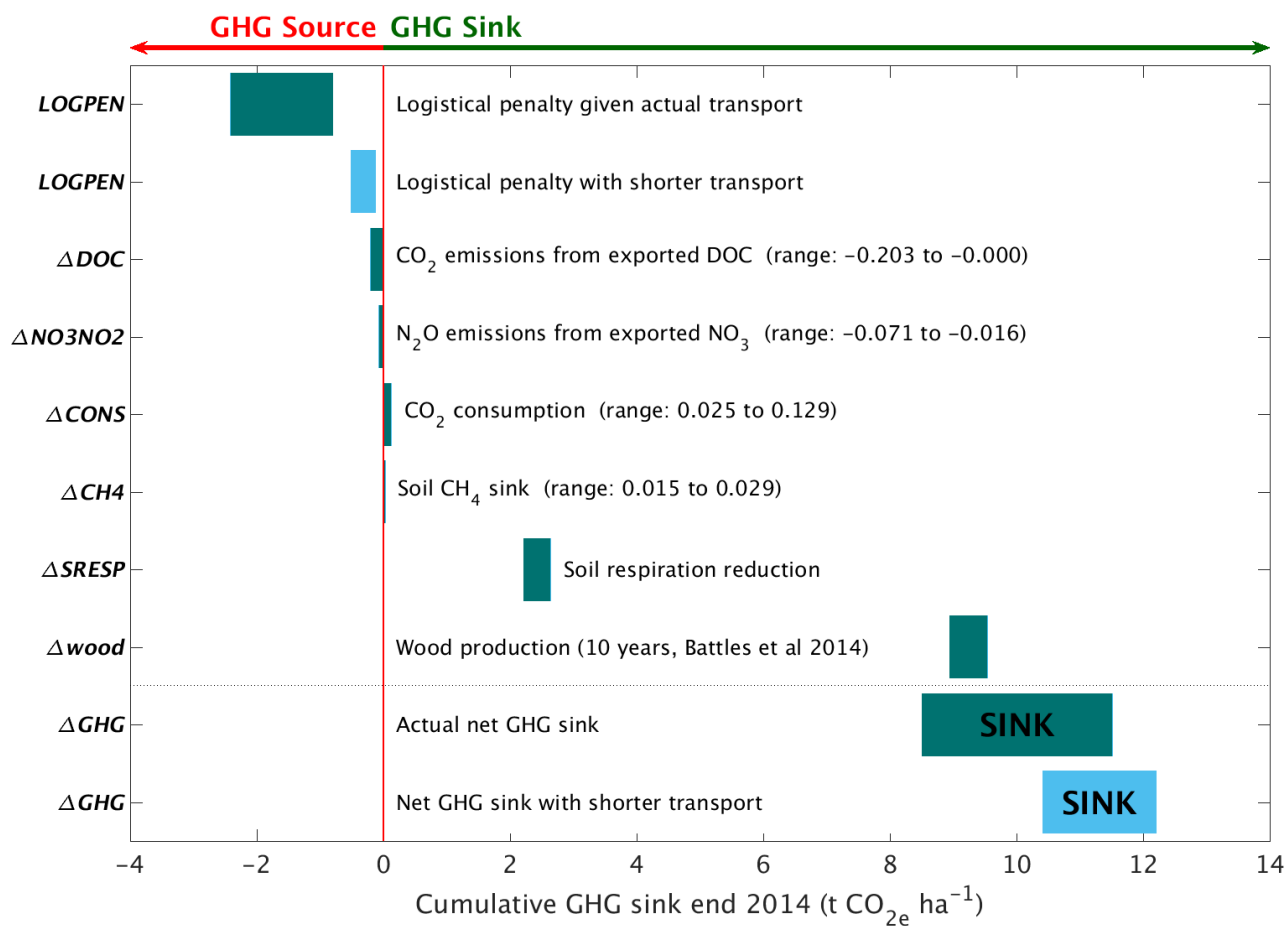
406 <sup>e</sup>The “optimistic” value for DOC assumes complete burial and undesirable low oxygen conditions in downstream waters.

407

408

409 These carbon emission penalties must be subtracted from watershed carbon removal to calculate net CDR for the  
 410 wollastonite treatment at HBEF (**Fig. 5; Table 4**). Compared in this way, we find increased wood production over ten years  
 411 (Battles et al., 2014) repays the total logistical CO<sub>2</sub> costs 4–12 times over. The components (**Fig. 5; Table 4**) comprise 8.5–  
 412 11.5 tCO<sub>2</sub> ha<sup>-1</sup> of the total GHG budget associated with the wollastonite treatment (Methods). These figures would increase  
 413 to 10.4–12.2 tCO<sub>2</sub> ha<sup>-1</sup> if the wollastonite had been pelletized anywhere along the route from Gouverneur to New Hampshire.

414 Wollastonite treatment effects on streamwater chemistry play a minor role in the greenhouse gas budget (**Fig. 5;**  
 415 **Table 4**). For our hypothetical ten-fold higher treatment ( $34.4 \text{ t ha}^{-1}$ ),  $\text{CO}_2$  consumption calculated by assumed calcium release  
 416 is  $\sim 10$  times higher, but carbon emission penalties scale with increased rock mass. Assuming pelletization near the mine to  
 417 reduce transport costs, the total logistical penalty would be  $1.2\text{--}5.1 \text{ tCO}_2 \text{ ha}^{-1}$ . In total, net CDR would be  $6.8\text{--}12.4 \text{ tCO}_2 \text{ ha}^{-1}$   
 418 for the the ten-fold larger treatment if none of the other GHG fluxes changed. We have not attempted to extrapolate other forest  
 419 biomass and soil GHG fluxes or streamwater DOC and  $\text{NO}_3^-$  responses.  
 420



421  
 422  
 423 **Figure 5: Carbon responses for the wollastonite treatment.** Elements of the greenhouse gas balance associated with the wollastonite  
 424 treatment (**Table 4**). The  $\text{CO}_2$  consumption range is given by  $Wo\text{-CO}_{2,\text{HCO}_3}$  calculated by Eq. (3) and  $Wo\text{-CO}_{2,\text{Ca}}$  calculated by Eq. (4), time-  
 425 integrated from the application date through 2014. Nitrate export in streamwater leading to  $\text{N}_2\text{O}$  greenhouse gas emissions downstream and  
 426 a small increase in the soil  $\text{CH}_4$  sink have been converted to  $\text{CO}_2$ -equivalents (Methods). Exported DOC is assumed to be respired  
 427 downstream.

428  
 429

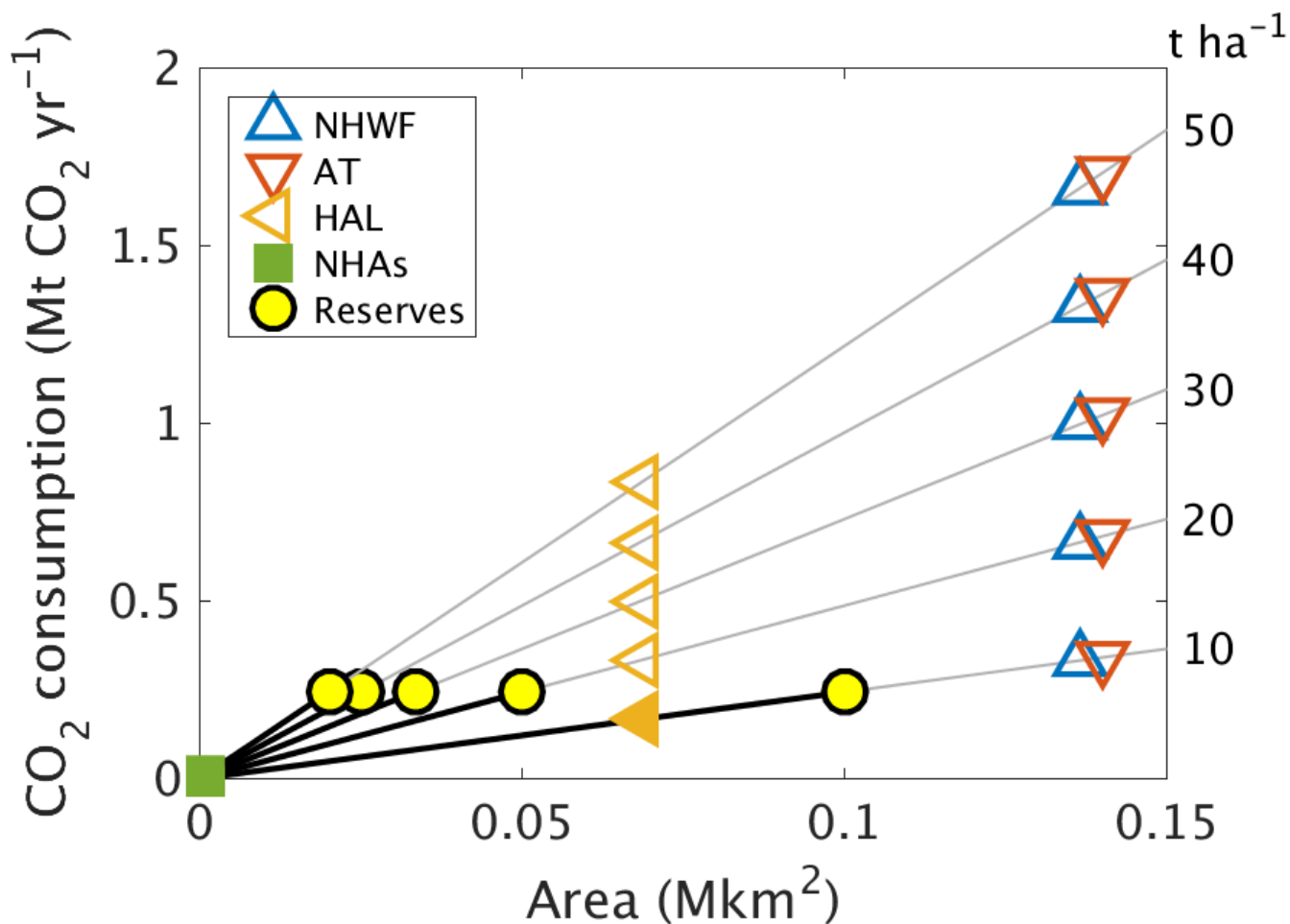
### 430 3.6 Potential for deployment at larger scales

431 The HBEF forests are representative of a major area of eastern North America receiving acid deposition since the 1950s  
432 (Likens and Bailey, 2014) which may be suitable for remediation and carbon capture via ERW treatment with a silicate rock  
433 or mineral. For example, the Appalachian and Laurentian-Acadian Northern Hardwood Forests (NHWF) covering a combined  
434 area of 0.137 Mkm<sup>2</sup> in the United States (Ferree and Anderson, 2013) have the same dominant hardwood trees as the HBEF  
435 experimental watersheds (*Fagus grandifolia*, *Betula allegheniensis* and *Acer saccharum*). Acid deposition exceeded “critical  
436 loads” likely to harm ecosystems in almost 9000 ha of New Hampshire’s *Acer saccharum* stands (NHAs) (Schaberg et al.,  
437 2010). These forests might be expected to respond similarly to a wollastonite treatment. The acid-sensitive trees *Acer*  
438 *saccharum* and *Picea rubens* are also widely distributed along the high elevation acid sensitive regions of the Appalachian  
439 Mountains which have already been impacted by acid deposition (Lawrence et al., 2015). We define this as a 40-km corridor  
440 along the Appalachian Mountains comprising 0.14 Mkm<sup>2</sup> and overlapping with the High Allegheny Plateau Ecoregion (HAL)  
441 where *Acer saccharum* is declining above ~550 m a.s.l. (Bailey et al., 2004) (0.07 Mkm<sup>2</sup>).

442 We examined the potential CO<sub>2</sub> consumption for a range of wollastonite application rates encompassing those suggested  
443 for ERW strategies (Strefler et al., 2018; Beerling et al., 2018) (Fig. 6). In this analysis, we adjusted mean (2003–2012) Wo-  
444 CO<sub>2,ca</sub> for the actual 3.44 t ha<sup>-1</sup> treatment (~0.2 mol C m<sup>-2</sup> yr<sup>-1</sup>) proportionally for 10–50 t ha<sup>-1</sup> treatments. We assume logistical  
445 carbon penalties are minimised and balanced by forest biomass carbon sequestration responses to treatment. This analysis  
446 suggests net CDR potential of 0.3–1.7 Mt CO<sub>2</sub> yr<sup>-1</sup> along the Appalachian corridor, which is 2–12% of New Hampshire state  
447 emissions (13.8 Mt CO<sub>2</sub>) in 2016 (Energy Information Administration, 2019). However, world wollastonite reserves (Curry,  
448 2019) (≥0.1 Pg) are insufficient to treat large areas of eastern North America at rates of 10–50 t ha<sup>-1</sup>, highlighting the  
449 requirement for alternative sustainable sources of silicate materials.

450

451



452

453 **Figure 6: Projected CO<sub>2</sub> consumption following higher-dosage treatments.** We considered the possibility of higher-dosage silicate  
 454 treatments on other northeastern United States higher-altitude forests affected by acid rain, such as *Acer saccharum* forests in New Hampshire  
 455 (NHAs), the High Allegheny Plateau Ecoregion (HAL), the Appalachian trail corridor (AT), or Northern Hardwood forests (NHWF)  
 456 dominated by the same tree species as at Hubbard Brook. Because the world's wollastonite reserves (yellow disks) are insufficient to treat  
 457 these areas, other calcium-rich silicate minerals would be required. CO<sub>2</sub> consumption due to higher dosage (t ha<sup>-1</sup>) is estimated as: (mean  
 458 observed CO<sub>2,Ca</sub> between 2004 and 2012) × area × dosage / 3.44 t ha<sup>-1</sup>.

459

#### 460 4 Discussion

461 Our analyses of wollastonite application at the HBEF provide a unique long-term (15 year) perspective on the whole watershed  
 462 carbon cycle responses and net CDR by accounting for the associated CO<sub>2</sub> costs of logistical operations. By 2015, net CDR  
 463 amounted to 8.5–11.5 t CO<sub>2</sub> ha<sup>-1</sup> at a low rate of wollastonite application, with increased carbon sequestration into forest  
 464 biomass playing the dominant role. We estimate that if the HBEF application rates were increased ten-fold, net CDR would

465 increase by 8%, assuming 400-km transport distances and no change in forest responses. Amplification of organic carbon  
466 capture may therefore represent a major CDR benefit of ERW when applied to forested lands affected by acid rain. Forest  
467 management practices, disturbance regimes and the ultimate fate of any harvested wood are also important in determining the  
468 storage lifetime of the sequestered carbon. Our results highlight the need to carefully monitor the net carbon balance of forested  
469 ecosystems in response to a silicate treatment, including wood and canopy respiration (Fahey et al., 2005) (Methods). This  
470 challenging goal might best be achieved with fully instrumented eddy covariance plots, although the HBEF topography is not  
471 well suited for this approach (Fahey et al., 2005).

472 Inorganic CO<sub>2</sub> consumption calculated based on streamwater bicarbonate fluxes approximately doubled in the treated  
473 watershed relative to the reference watershed 15 years post-treatment (0.028 and 0.016 tCO<sub>2</sub> ha<sup>-1</sup>, respectively) (**Table 3**). The  
474 presence of SO<sub>4</sub><sup>2-</sup>, NO<sub>3</sub><sup>-</sup> and organic acid anions lowered the efficiency of CO<sub>2</sub> consumption by alkalinity generation, with acid  
475 deposition having the single largest calculated effect (**Table 3**). The cause of increased NO<sub>3</sub><sup>-</sup> export from the treated watershed  
476 is not as yet understood (Rosi-Marshall et al., 2016). If it proves a general feature of terrestrial ecosystem responses to silicate  
477 mineral treatment, this could affect the efficiency of carbon capture via bicarbonate export. Overall, we suggest that continued  
478 recovery of eastern North American and European forests and soils from acid deposition creates conditions beneficial to  
479 watershed health, carbonic acid-driven weathering and inorganic carbon export following application of crushed silicate  
480 minerals.

481 In Asia, acid rain is an ongoing problem with an estimated 28% of Chinese land area (~2.7 Mkm<sup>2</sup>) receiving potentially  
482 damaging S deposition in 2005 (Zhao et al., 2009), and critical loads were exceeded in ~0.36 Mkm<sup>2</sup> of the European Economic  
483 Area (EEA) in 1999 (Larssen et al., 2003), approximately double the affected area of US Northern Hardwood Forests (**Fig. 6**).  
484 **Fig. 6** suggests that a single 30t Wo ha<sup>-1</sup> treatment over 0.14 Mkm<sup>2</sup> (Appalachian Trail corridor) could, in principle, sequester  
485 ~1 MtCO<sub>2</sub> y<sup>-1</sup> or 15 MtCO<sub>2</sub> over 15 years via wollastonite-derived Ca export in streamwater alone. Adding the Chinese and  
486 European acidified areas could potentially sequester 0.34 GtCO<sub>2</sub>, approximately 0.2–0.7% of the ~50–150 Gt CDR required  
487 by 2050 to avoid warming in excess of 1.5° (Rogelj et al., 2018). Inclusion of biomass and soil responses increases CDR  
488 contributions from ERW on acidified forests, but these will still be modest. Assuming no further forest responses beyond the  
489 15-year HBEF timeframe, we report a GHG balance of ~10 tCO<sub>2e</sub> ha<sup>-1</sup>. This translates to 1 GtCO<sub>2e</sub> Mkm<sup>-2</sup> suggesting 3.2  
490 GtCO<sub>2e</sub> over 15 years for the Appalachian Trail, the EEA and China combined, or 2–6% of global required CDR as described  
491 above.

492 It is uncertain whether other acidified forest ecosystems would respond similarly to the HBEF *Acer saccharum* forests  
493 in New Hampshire. Many Chinese soils (Duan et al., 2016), as well as old deep soils in areas such as the Virginian Blue Ridge  
494 Mountains and the German Harz and Fetchel Mountains (Garmo et al., 2014), have high SO<sub>4</sub><sup>2-</sup> sorption capacity. These soils  
495 may retain substantially more SO<sub>4</sub><sup>2-</sup> than the HBEF soils, with potential for prolonged SO<sub>4</sub><sup>2-</sup> flushing following ERW treatment  
496 and lower bicarbonate production. Liming studies suggest a range of other effects, some of which may also occur with silicate  
497 treatments. Liming increases nitrate export, migration of heavy metals and acidity to deeper soil, and fine root production in  
498 topsoils leading to frost damage (Huettl and Zoettl, 1993).



499 Many forests have been limed with carbonate minerals such as calcite and dolomite to mitigate acidification in the past.  
500 Dolomite has also helped reverse Mg deficiency in conifers (Huettl and Zoettl, 1993). Liming generally improves water  
501 quality, although it also forms mixing zones with high-molecular-weight Al complexes toxic to fish (Teien et al., 2006). With  
502 silicate treatments, nontoxic hydroxyaluminosilicates form instead (Teien et al., 2006). Unfortunately, carbonates are  
503 contraindicated for CDR on acid soils because they can be a net source of CO<sub>2</sub> in the presence of strong acids (Hamilton et al.,  
504 2007). Treatments of European and North American acidified forests with calcite (1–18 t ha<sup>-1</sup> CaCO<sub>3</sub>) or dolomite (2–8.7 t  
505 ha<sup>-1</sup> CaMg(CO<sub>3</sub>)<sub>2</sub>) have, in general, resulted in increased DOC export and soil respiration without increasing tree growth,  
506 regardless of forest composition (Lundström et al., 2003). As calcite and dolomite are 44% and 48% CO<sub>2</sub> by weight, these  
507 treatments will have released 0.44–7.9 and 0.96–4.54 t CO<sub>2</sub> ha<sup>-1</sup> respectively when fully dissolved, although dissolution may  
508 be slow. Over six years following a 2.9 t dolomite ha<sup>-1</sup> treatment (90% 0.2–2.0 mm grains) in a Norwegian coniferous  
509 watershed equating to 1.36 t CO<sub>2</sub> ha<sup>-1</sup>, less than 1% of the dolomite dissolved (Hindar et al., 2003). We estimate that CO<sub>2</sub>  
510 consumption corrected for CO<sub>2</sub> release and as measured with dolomite-derived Ca and Mg in streamwater (Dol-CO<sub>2,Ca+Mg</sub>)  
511 averaged 0.02 mol CO<sub>2</sub> m<sup>-2</sup> yr<sup>-1</sup>. CO<sub>2</sub> release from carbonate minerals equals Ca and Mg release on a molar basis, so 0.02 mol  
512 Dol-CO<sub>2</sub> m<sup>-2</sup> yr<sup>-1</sup> was also either exported in streamwater or lost to the atmosphere. This experiment may have a negative  
513 greenhouse-gas balance depending on logistical penalties and soil respiration, as there was no significant treatment effect on  
514 tree growth or vitality (Hindar et al., 2003). Ca-sensitive *Acer saccharum* is present at Woods Lake in New York State, yet  
515 tree biomass decreased with no significant differences relative to reference catchments during the 20 years following a 6.89 t  
516 Mg-calcite ha<sup>-1</sup> application (Melvin et al., 2013), equivalent to 3.07 t CO<sub>2</sub> ha<sup>-1</sup> given 8% Mg content of the pellets. In contrast  
517 to our study and other liming studies, root biomass and soil carbon stocks increased in response to this treatment, although soil  
518 respiration was reduced (Melvin et al., 2013). *Acer saccharum* basal area and crown vigour increased over 23 years in response  
519 to 22.4 t dolomitic limestone ha<sup>-1</sup> (equivalent to 10.0 t CO<sub>2</sub> ha<sup>-1</sup>) on the Allegheny Plateau, although basal area and survival of  
520 another dominant canopy species, *Prunus serotina*, was reduced (Long et al., 2011). Clearly, forest responses to mineral  
521 treatments are species- and site-specific.

522 Although the HBEF experiment used wollastonite, this is not a target mineral for ERW, both because of its limited  
523 reserves (Curry, 2019) and high monetary costs (Schlesinger and Amundson, 2018). Recent all-inclusive guide prices of ~700  
524 USD Mg<sup>-1</sup> for helicopter deployment of pelletized lime along the Appalachian Mountain corridor are comparable to the price  
525 of 694 USD Mg<sup>-1</sup> for unpelletized 10-μm wollastonite in 2000 (Virta, 2000). Less expensive materials such as locally-sourced  
526 waste fines from mines or volcanic ash (Longman et al., 2020) should be considered if their heavy metal content is low, but  
527 the choice of treatment material should be considered together with the vegetation and the native minerals. Application of  
528 magnesium-rich materials (e.g. olivine), for example, may help reverse Mg deficiency in *Pinus sylvatica* and *Picea abies* as  
529 dolomite has done (Huettl and Zoettl, 1993), but some other tree species, such as *Acer saccharum*, have a higher demand for  
530 calcium than for magnesium (Long et al., 2009). The treatment of ecologically sensitive catchments always requires caution  
531 as some species, such as *Sphagnum* mosses and lichens, may respond poorly to treatment (Traaen et al., 1997).

532 Finally, we consider integration of ERW treatments with forest management practices. Dominant CDR pathways  
 533 depend on biogeochemical cycling which in turn depends on the life cycle of the dominant trees. For example, base cation  
 534 export and therefore CO<sub>2</sub> consumption temporarily increases following clear-felling, then decreases while trees are young and  
 535 growing due to base cation uptake, and remains low after trees mature due to nutrient recycling (Balogh-Brunstad et al., 2008).  
 536 These dynamics may be less obvious in forests which are not clear-felled; *Acer saccharum* forests are often thinned and retain  
 537 a canopy as the seedlings are adapted to shade. Individual *Acer saccharum* trees can live for over 300 years, growing relatively  
 538 slowly for the first 40 years and attaining maximum height during the first 150 years (Godman et al., 1990). One may expect  
 539 to maximise wood production of growing trees with ERW treatments meeting or exceeding the forest demand for previously  
 540 limited nutrients such as calcium, which would also minimise soil respiration if the trees allocate less carbon to roots.  
 541 Treatments could be repeated as necessary to meet the nutritional needs of sensitive trees or to maintain high CO<sub>2</sub> consumption.  
 542 Conversely, rising soil pH may not suit some species. For example, *Acer saccharum* normally grows in organic-rich soils with  
 543 pH under 7.3 (Godman et al., 1990) and its growth may be hindered at higher pH following large treatments. Outside the main  
 544 tree growth phase, and in forests without responsive tree species, CO<sub>2</sub> consumption could become the dominant GHG response  
 545 to ERW treatments depending on the extent to which it is counteracted by DOC export as soil pH rises (Johnson et al., 2014)  
 546 and decomposition rates and fluxes rise (Lovett et al., 2016). Site-specific research is required to determine the optimum  
 547 dosage, timing, efficacy and suitability of ERW treatments on acid-impacted forests.

548

#### 549 **Appendix A Contributions of rain/snow precipitation to streamwater chemistry**

550 We estimated the contribution of rain/snow (Likens, 2016b, a) relative to all other sources using a previously published mixing  
 551 model (Négrel et al., 1993). We assume all Cl<sup>-</sup> in the water is from rain/snow, noting however that this common treatment of  
 552 Cl as an unreactive tracer is not always justified (Lovett et al., 2005). We calculate the contribution of precipitation to the  
 553 streamwater ( $\alpha_{\text{rain}}$ ) using Na and Cl, which are less affected by nutrient cycling and adsorption than other major ions (Négrel  
 554 et al., 1993):

$$555 \quad \alpha_{\text{rain,Na}}(\mathbf{t}) = \frac{\left[\frac{\text{Cl}}{\text{Na}}\right](\text{stream},\mathbf{t})}{\left[\frac{\text{Cl}}{\text{Na}}\right](\text{rain},\mathbf{t})}, \quad (\text{A1})$$

556

557 To account for attenuation of the rain/snow precipitation leaching through the soil, Cl/Na and HCO<sub>3</sub><sup>-</sup>/Na at any given time ( $\mathbf{t}$ )  
 558 are means from the previous three months. We estimate the contribution of rain/snow to other ions such as HCO<sub>3</sub><sup>-</sup> in the  
 559 streamwater as follows:

$$560 \quad \alpha_{\text{rain,HCO}_3}(\mathbf{t}) = \alpha_{\text{rain,Na}}(\mathbf{t}) \times \frac{\left[\frac{\text{HCO}_3}{\text{Na}}\right](\text{stream},\mathbf{t})}{\left[\frac{\text{HCO}_3}{\text{Na}}\right](\text{rain},\mathbf{t})}, \quad (\text{A2})$$

## 561 **Appendix B Fraction of calcium derived from wollastonite**

562 We applied an existing two-component mixing model (Peters et al., 2004):

$$563 \quad X_{Ca}(t) = \left[ \frac{\left( \left( \frac{^{87}\text{Sr}}{^{86}\text{Sr}} \right)_{\text{post}} - \left( \frac{^{87}\text{Sr}}{^{86}\text{Sr}} \right)_{\text{pre}} \right) \left( \frac{\text{Sr}}{\text{Ca}} \right)_{\text{pre}}}{\left( \left( \frac{^{87}\text{Sr}}{^{86}\text{Sr}} \right)_{\text{post}} - \left( \frac{^{87}\text{Sr}}{^{86}\text{Sr}} \right)_{\text{pre}} \right) \left( \frac{\text{Sr}}{\text{Ca}} \right)_{\text{pre}} + \left( \left( \frac{^{87}\text{Sr}}{^{86}\text{Sr}} \right)_{\text{Wo}} - \left( \frac{^{87}\text{Sr}}{^{86}\text{Sr}} \right)_{\text{pre}} \right) \left( \frac{\text{Sr}}{\text{Ca}} \right)_{\text{Wo}}} \right], \quad (B1)$$

564 where pre-app and post-app refer to pre-application and post-application streamwater concentrations and Wo refers to  
565 wollastonite. The Sr data (Blum, 2019) have been extended through 2015 (**Fig. S1a**). See Supplementary Information for  
566 further discussion of the use of strontium and its isotopes as tracers of  $\text{Ca}^{2+}$  provenance.

567

568

### 569 **Code availability**

570 The aqueous geochemistry software PHREEQC software, along with documentation, is freely available from the USGS  
571 website (<https://www.usgs.gov/software/phreeqc-version-3>). MATLAB<sup>®</sup> may be purchased from the MathWorks website  
572 (<https://uk.mathworks.com/products/matlab.html>). Our MATLAB code and scripts used for this project are provided in a  
573 supplementary .zip file, without guarantees that these will run with MATLAB versions other than R2016a or on non-Linux  
574 operating systems.

### 575 **Data availability**

576 Our data are available from the Long Term Ecological Research (LTER) Network Data Portal. This public repository can be  
577 accessed via the Hubbard Brook Ecosystem Study website: <https://hubbardbrook.org/d/hubbard-brook-data-catalog>

578 See Supplement for a full list of filenames, package IDs, DOIs and access dates.

### 579 **Author contributions**

580 All authors contributed to project conceptualization and interpretation of model results. L.L.T. undertook model simulations  
581 and data analysis. L.L.T. and D.J.B. drafted the manuscript with edits and revisions from all authors. C.T.D. designed the  
582 wollastonite watershed study, provided data and observations for model simulations. J.D.B. provided strontium isotope  
583 datasets. P.M.G. provided soil respiration, nitrous oxide and methane flux data.

584 **Competing interests**

585 The authors declare that they have no conflict of interest.

586 **Disclaimer**

587 **Acknowledgements**

588 L.L.T. and D.J.B. gratefully acknowledge funding from the Leverhulme Trust through a Leverhulme Research Centre Award  
589 (RC-2015-029). This manuscript is a contribution of the Hubbard Brook Ecosystem Study. Hubbard Brook is part of the Long-  
590 Term Ecological Research (LTER) network, which is supported by the National Science Foundation (DEB-1633026). L.L.T.  
591 thanks Ruth Yanai for a helpful discussion about vegetation, Fred Worrall for advice on flow adjustment and flux calculation,  
592 Peter Wade for advice on the initial PHREEQC setup and Andrew Beckerman and Evan DeLucia for constructive criticism  
593 and advice on statistical modelling. We are grateful to Gregory Lawrence for information about applying lime treatments to  
594 the Appalachian Trail corridor, to Lisa Martel for providing the locations of the trace gas sampling sites and to Habibollah  
595 Fahkraei for creating the watershed map with weir and trace gas sampling locations in Fig. 1. We are grateful for comments  
596 from W. Brian Whalley and editor Tyler Cyronak, and for reviews from Morgan Jones and an anonymous referee which led  
597 to major improvements in this manuscript.

598 **References**

- 599 Bailey, S., Horsley, S., Long, R., and Hallett, R.: Influence of edaphic factors on sugar maple nutrition and health on the  
600 Allegheny Plateau, *Soil Science Society of America Journal*, 68, 243–252, 2004.
- 601 Balogh-Brunstad, Z., Keller, C. K., Bormann, B. T., O'Brien, R., Wang, D., and Hawley, G.: Chemical weathering and  
602 chemical denudation dynamics through ecosystem development and disturbance, *Global Biogeochemical Cycles*, 22, GB1007,  
603 10.1029/2007GB002957, 2008.
- 604 Battles, J. J., Fahey, T. J., Driscoll Jr, C. T., Blum, J. D., and Johnson, C. E.: Restoring soil calcium reverses forest decline,  
605 *Environmental Science & Technology Letters*, 1, 15–19, 2014.
- 606 Battles, J. J., Driscoll Jr, C. T., Bailey, S. W., Blum, J. D., Buso, D. C., Fahey, T. J., Fisk, M., Groffman, P. M., Johnson, C.,  
607 and Likens, G.: Forest Inventory of a Calcium Amended Northern Hardwood Forest: Watershed 1, 2011, Hubbard Brook  
608 Experimental Forest. Environmental Data Initiative, 10.6073/pasta/94f9084a3224c1e3e0ed38763f8dae02, 2015a.
- 609 Battles, J. J., Driscoll Jr, C. T., Bailey, S. W., Blum, J. D., Buso, D. C., Fahey, T. J., Fisk, M., Groffman, P. M., Johnson, C.,  
610 and Likens, G.: Forest Inventory of a Calcium Amended Northern Hardwood Forest: Watershed 1, 2006, Hubbard Brook  
611 Experimental Forest. Environmental Data Initiative, 10.6073/pasta/37c5a5868158e87db2d30c2d62a57e14, 2015b.
- 612 Beerling, D. J., Leake, J. R., Long, S. P., Scholes, J. D., Ton, J., Nelson, P. N., Bird, M., Kantzas, E., Taylor, L. L., and Sarkar,  
613 B.: Farming with crops and rocks to address global climate, food and soil security, *Nature plants*, 4, 138–147, 2018.
- 614 Blum, J. D., Klaue, A., Nezat, C. A., Driscoll, C. T., Johnson, C. E., Siccama, T. G., Eagar, C., Fahey, T. J., and Likens, G.  
615 E.: Mycorrhizal weathering of apatite as an important calcium source in base-poor forest ecosystems, *Nature*, 417, 729–731,  
616 2002.
- 617 Blum, J. D.: Streamwater Ca, Sr and  $^{87}\text{Sr}/^{86}\text{Sr}$  measurements on Watershed 1 at the Hubbard Brook Experimental Forest.  
618 Environmental Data Initiative, 10.6073/pasta/43ebc0f959780cfc30b7ad53cc4a3d3e, 2019.

619 Brantley, S. L., Kubicki, J. D., and White, A. F.: Kinetics of water-rock interaction, 2008.

620 Campbell, J.: Hubbard Brook Experimental Forest (USDA Forest Service): Daily Streamflow by Watershed, 1956–present,  
621 Environmental Data Initiative, 10.6073/pasta/727ee240e0b1e10c92fa28641bedb0a3, 2015.

622 Campbell, J.: Hubbard Brook Experimental Forest (USDA Forest Service): Daily Mean Temperature Data, 1955–present.  
623 Environmental Data Initiative, 10.6073/pasta/75b416d670de920c5ace92f8f3182964, 2016.

624 Campbell, J. L., Driscoll, C. T., Eagar, C., Likens, G. E., Siccama, T. G., Johnson, C. E., Fahey, T. J., Hamburg, S. P., Holmes,  
625 R. T., and Bailey, A. S.: Long-term trends from ecosystem research at the Hubbard Brook Experimental Forest, Gen. Tech.  
626 Rep. NRS-17. Newtown Square, PA: US Department of Agriculture, Forest Service, Northern Research Station. 41 p., 17,  
627 2007.

628 Campbell, J. L., Rustad, L. E., Boyer, E. W., Christopher, S. F., Driscoll, C. T., Fernandez, I. J., Groffman, P. M., Houle, D.,  
629 Kiebusch, J., and Magill, A. H.: Consequences of climate change for biogeochemical cycling in forests of northeastern North  
630 America, *Canadian Journal of Forest Research*, 39, 264–284, 2009.

631 Cawley, K. M., Campbell, J., Zwilling, M., and Jaffé, R.: Evaluation of forest disturbance legacy effects on dissolved organic  
632 matter characteristics in streams at the Hubbard Brook Experimental Forest, New Hampshire, *Aquatic sciences*, 76, 611–622,  
633 2014.

634 Chetelat, B., Liu, C.-Q., Zhao, Z., Wang, Q., Li, S., Li, J., and Wang, B.: Geochemistry of the dissolved load of the Changjiang  
635 Basin rivers: anthropogenic impacts and chemical weathering, *Geochimica et Cosmochimica Acta*, 72, 4254–4277, 2008.

636 Cho, Y., Driscoll, C. T., Johnson, C. E., Blum, J. D., and Fahey, T. J.: Watershed-level responses to calcium silicate treatment  
637 in a northern hardwood forest, *Ecosystems*, 15, 416–434, 2012.

638 Mineral Commodity Summaries: Wollastonite: <https://www.usgs.gov/centers/nmic/wollastonite-statistics-and-information>,  
639 access: 11 September, 2019.

640 De Klein, C., Novoa, R. S., Ogle, S., Smith, K. A., Rochette, P., Wirth, T. C., McConkey, B. G., Mosier, A., Rypdal, K., and  
641 Walsh, M.: N<sub>2</sub>O emissions from managed soils, and CO<sub>2</sub> emissions from lime and urea application, IPCC guidelines for  
642 National greenhouse gas inventories, prepared by the National greenhouse gas inventories programme, 4, 1–54, 2006.

643 Driscoll, C. T., Bailey, S. W., Blum, J. D., Buso, D. C., Eagar, C., Fahey, T. J., Fisk, M., Groffman, P. M., Johnson, C., Likens,  
644 G., Hamburg, S. P., and Siccama, T. G.: Forest Inventory of a Calcium Amended Northern Hardwood Forest: Watershed 1,  
645 2001, Hubbard Brook Experimental Forest. Environmental Data Initiative,  
646 10.6073/pasta/a2300121b6d594bbfcb3256ca1c300c8, 2015.

647 Driscoll, C. T.: Longitudinal Stream Chemistry at the Hubbard Brook Experimental Forest, Watershed 1, 1991–present.  
648 Environmental Data Initiative, 10.6073/pasta/fcfa498c5562ee55f6e84d7588a980d2, 2016a.

649 Driscoll, C. T.: Longitudinal Stream Chemistry at the Hubbard Brook Experimental Forest, Watershed 6, 1982–present.  
650 Environmental Data Initiative, 10.6073/pasta/0033e820ff0e6a055382d4548dc5c90c, 2016b.

651 Driscoll Jr, C. T., Bailey, S. W., Blum, J. D., Buso, D. C., Eagar, C., Fahey, T. J., Fisk, M., Groffman, P. M., Johnson, C.,  
652 Likens, G., Hamburg, S. P., and Siccama, T. G.: Forest Inventory of a Calcium Amended Northern Hardwood Forest:  
653 Watershed 1, 1996, Hubbard Brook Experimental Forest. Environmental Data Initiative,  
654 10.6073/pasta/9ff720ba22aef2b40fc5d9a7b374aa52, 2015.

655 Duan, L., Yu, Q., Zhang, Q., Wang, Z., Pan, Y., Larssen, T., Tang, J., and Mulder, J.: Acid deposition in Asia: emissions,  
656 deposition, and ecosystem effects, *Atmospheric Environment*, 146, 55–69, 10.1016/j.atmosenv.2016.07.018, 2016.

657 Energy Information Administration: Inventory of Power Plants in the United States, United States Department of Energy,  
658 Washington, DCDOE/EIA-0095(97), 431, 1997.

659 Energy Information Administration: Energy-Related Carbon Dioxide Emissions by State, 2005–2016, United States  
660 Department of Energy, Washington DC 20585, 34, 2019.

661 Fahey, T., Siccama, T., Driscoll, C., Likens, G., Campbell, J., Johnson, C., Battles, J., Aber, J., Cole, J., and Fisk, M.: The  
662 biogeochemistry of carbon at Hubbard Brook, *Biogeochemistry*, 75, 109–176, 2005.

663 Fahey, T. J., Heinz, A. K., Battles, J. J., Fisk, M. C., Driscoll, C. T., Blum, J. D., and Johnson, C. E.: Fine root biomass declined  
664 in response to restoration of soil calcium in a northern hardwood forest, *Canadian Journal of Forest Research*, 46, 738–744,  
665 2016.

666 Fakhraei, H., and Driscoll, C. T.: Proton and aluminum binding properties of organic acids in surface waters of the northeastern  
667 US, *Environmental science & technology*, 49, 2939–2947, 2015.

668 Fakhraei, H., Driscoll, C. T., Renfro, J. R., Kulp, M. A., Blett, T. F., Brewer, P. F., and Schwartz, J. S.: Critical loads and  
669 exceedances for nitrogen and sulfur atmospheric deposition in Great Smoky Mountains National Park, United States,  
670 *Ecosphere*, 7, e01466, 2016.

671 Ferree, C., and Anderson, M. G.: A map of terrestrial habitats of the Northeastern United States: methods and approach, *Nature*  
672 *Conservancy*, 10, 31, 2013.

673 Fuller, R., Driscoll, C., Lawrence, G., and Nodvin, S.: Processes regulating sulphate flux after whole-tree harvesting, *Nature*,  
674 325, 707–710, 1987.

675 Garmo, Ø. A., Skjelkvåle, B. L., de Wit, H. A., Colombo, L., Curtis, C., Fölster, J., Hoffmann, A., Hruška, J., Høgåsen, T.,  
676 and Jeffries, D. S.: Trends in surface water chemistry in acidified areas in Europe and North America from 1990 to 2008,  
677 *Water, Air, & Soil Pollution*, 225, 1880, 10.1007/s11270-014-1880-6, 2014.

678 Godman, R. M., Yawney, H. W., and Tubbs, C. H.: *Acer saccharum* Marsh. sugar maple, *Silvics of North America*, 2, 1990.

679 Goodale, C. L., and Aber, J. D.: The long-term effects of land-use history on nitrogen cycling in northern hardwood forests,  
680 *Ecological Applications*, 11, 253–267, 2001.

681 Groffman, P. M., Fisk, M. C., Driscoll, C. T., Likens, G. E., Fahey, T. J., Eagar, C., and Pardo, L. H.: Calcium additions and  
682 microbial nitrogen cycle processes in a northern hardwood forest, *Ecosystems*, 9, 1289–1305, 2006.

683 Groffman, P. M.: Forest soil: atmosphere fluxes of carbon dioxide, nitrous oxide and methane at the Hubbard Brook  
684 Experimental Forest, 1997–present. Environmental Data Initiative, 10.6073/pasta/9d017f1a32cba6788d968dc03632ee03,  
685 2016.

686 Hamilton, S. K., Kurzman, A. L., Arango, C., Jin, L., and Robertson, G. P.: Evidence for carbon sequestration by agricultural  
687 liming, *Global Biogeochemical Cycles*, 21, GB2021, 10.1029/2006GB002738, 2007.

688 Harrison, R. B., Johnson, D. W., and Todd, D. E.: Sulfate adsorption and desorption reversibility in a variety of forest soils,  
689 *Journal of Environmental Quality*, 18, 419–426, 1989.

690 Hartmann, J., West, A. J., Renforth, P., Köhler, P., Christina, L., Wolf-Gladrow, D. A., Dürr, H. H., and Scheffran, J.: Enhanced  
691 chemical weathering as a geoengineering strategy to reduce atmospheric carbon dioxide, supply nutrients, and mitigate ocean  
692 acidification, *Reviews of Geophysics*, 51, 113–149, 2013.

693 Hindar, A., Wright, R. F., Nilsen, P., Larssen, T., and Høgberget, R.: Effects on stream water chemistry and forest vitality after  
694 whole-catchment application of dolomite to a forest ecosystem in southern Norway, *Forest Ecology and Management*, 180,  
695 509–525, 2003.

696 Hu, M., Chen, D., and Dahlgren, R. A.: Modeling nitrous oxide emission from rivers: a global assessment, *Global change*  
697 *biology*, 22, 3566–3582, 2016.

698 Huettl, R. F., and Zoettl, H.: Liming as a mitigation tool in Germany's declining forests—reviewing results from former and  
699 recent trials, *Forest Ecology and Management*, 61, 325–338, 1993.

700 Jacobson, A. D., and Blum, J. D.: Relationship between mechanical erosion and atmospheric CO<sub>2</sub> consumption in the New  
701 Zealand Southern Alps, *Geology*, 31, 865–868, 2003.

702 Johnson, C. E., Driscoll, C. T., Blum, J. D., Fahey, T. J., and Battles, J. J.: Soil chemical dynamics after calcium silicate  
703 addition to a northern hardwood forest, *Soil Science Society of America Journal*, 78, 1458–1468, 2014.

704 Johnson, N. M., Driscoll, C. T., Eaton, J. S., Likens, G. E., and McDowell, W. H.: ‘Acid rain’, dissolved aluminum and  
705 chemical weathering at the Hubbard Brook Experimental Forest, New Hampshire, *Geochimica et Cosmochimica Acta*, 45,  
706 1421–1437, 1981.

707 Köhler, S., Laudon, H., Wilander, A., and Bishop, K.: Estimating organic acid dissociation in natural surface waters using total  
708 alkalinity and TOC, *Water Research*, 34, 1425–1434, 2000.

709 Larssen, S., Barrett, K. J., Fiala, J., Goodwin, J., Hagen, L. O., Henriksen, J. F., de Leeuw, F., Tarrason, L., and van Aalst, R.:  
710 Air quality in Europe, 2003.

711 Lawrence, G., Sullivan, T., Burns, D., Bailey, S., Cosby, B., Dovciak, M., Ewing, H., McDonnell, T., Minocha, R., and Rice,  
712 K.: Acidic deposition along the Appalachian Trail corridor and its effects on acid-sensitive terrestrial and aquatic resources:  
713 results of the Appalachian Trail MEGA-transect atmospheric deposition effects study, National Park Service, Fort Collins,  
714 Colorado, 2015.

715 Likens, G.: Chemistry of Bulk Precipitation at Hubbard Brook Experimental Forest, Watershed 6, 1963–present.  
716 Environmental Data Initiative, 10.6073/pasta/8d2d88dc718b6c5a2183cd88aae26fb1, 2016a.

717 Likens, G.: Chemistry of Bulk Precipitation at Hubbard Brook Experimental Forest, Watershed 1, 1963–present.  
718 Environmental Data Initiative, 10.6073/pasta/df90f97d15c28daeb7620b29e2384bb9, 2016b.

719 Likens, G. E., Buso, D. C., Dresser, B. K., Bernhardt, E. S., Hall Jr, R. O., Macneale, K. H., and Bailey, S. W.: Buffering an  
720 acidic stream in New Hampshire with a silicate mineral, *Restoration Ecology*, 12, 419–428, 2004.

721 Likens, G. E.: Biogeochemistry of a forested ecosystem, 3 ed., Springer Science & Business Media, 208 pp., 2013.

722 Likens, G. E., and Bailey, S. W.: The discovery of acid rain at the Hubbard Brook Experimental Forest: a story of collaboration  
723 and long-term research, in: *USDA Forest Service Experimental Forests and Ranges*, Springer, 463–482, 2014.

724 Littlewood, I., Watts, C., and Custance, J.: Systematic application of United Kingdom river flow and quality databases for  
725 estimating annual river mass loads (1975–1994), *Science of the Total Environment*, 210, 21–40, 1998.

726 Long, R. P., Horsley, S. B., Hallett, R. A., and Bailey, S. W.: Sugar maple growth in relation to nutrition and stress in the  
727 northeastern United States, *Ecological Applications*, 19, 1454–1466, 2009.

728 Long, R. P., Horsley, S. B., and Hall, T. J.: Long-term impact of liming on growth and vigor of northern hardwoods, *Canadian  
729 Journal of Forest Research*, 41, 1295–1307, 2011.

730 Longman, J., Palmer, M. R., and Gernon, T. M. J. A.: Viability of greenhouse gas removal via the artificial addition of volcanic  
731 ash to the ocean, 100264, 2020.

732 Lovett, G. M., Likens, G. E., Buso, D. C., Driscoll, C. T., and Bailey, S. W.: The biogeochemistry of chlorine at Hubbard  
733 Brook, New Hampshire, USA, *Biogeochemistry*, 72, 191–232, 2005.

734 Lovett, G. M., Arthur, M. A., and Crowley, K. F.: Effects of calcium on the rate and extent of litter decomposition in a northern  
735 hardwood forest, *Ecosystems*, 19, 87–97, 2016.

736 Lundström, U., Bain, D., Taylor, A., and Van Hees, P.: Effects of acidification and its mitigation with lime and wood ash on  
737 forest soil processes: a review, *Water, Air and Soil Pollution: Focus*, 3, 5–28, 2003.

738 Martin, A. R., Doraisami, M., and Thomas, S. C.: Global patterns in wood carbon concentration across the world’s trees and  
739 forests, *Nature Geoscience*, 10.1038/s41561-018-0246-x, 2018.

740 McLaughlan, K. K., Craine, J. M., Oswald, W. W., Leavitt, P. R., and Likens, G. E.: Changes in nitrogen cycling during the  
741 past century in a northern hardwood forest, *Proceedings of the National Academy of Sciences*, 104, 7466–7470, 2007.

742 Melvin, A. M., Lichstein, J. W., and Goodale, C. L.: Forest liming increases forest floor carbon and nitrogen stocks in a mixed  
743 hardwood forest, *Ecological applications*, 23, 1962–1975, 2013.

744 Mohseni, O., and Stefan, H.: Stream temperature/air temperature relationship: a physical interpretation, *Journal of hydrology*,  
745 218, 128–141, 1999.

746 Moon, S., Chamberlain, C., and Hilley, G.: New estimates of silicate weathering rates and their uncertainties in global rivers,  
747 *Geochimica et Cosmochimica Acta*, 134, 257–274, 2014.

748 Moosdorf, N., Renforth, P., and Hartmann, J.: Carbon dioxide efficiency of terrestrial enhanced weathering, *Environmental  
749 science & technology*, 48, 4809–4816, 2014.

750 Négrel, P., Allègre, C. J., Dupré, B., and Lewin, E.: Erosion sources determined by inversion of major and trace element ratios  
751 and strontium isotopic ratios in river water: the Congo Basin case, *Earth and Planetary Science Letters*, 120, 59–76, 1993.

752 Nezat, C. A., Blum, J. D., and Driscoll, C. T.: Patterns of Ca/Sr and <sup>87</sup>Sr/<sup>86</sup>Sr variation before and after a whole watershed  
753 CaSiO<sub>3</sub> addition at the Hubbard Brook Experimental Forest, USA, *Geochimica et Cosmochimica Acta*, 74, 3129–3142,  
754 10.1016/j.gca.2010.03.013, 2010.

755 Pachauri, R. K., Allen, M. R., Barros, V. R., Broome, J., Cramer, W., Christ, R., Church, J. A., Clarke, L., Dahe, Q., and  
756 Dasgupta, P.: Climate change 2014: synthesis report. Contribution of Working Groups I, II and III to the fifth assessment  
757 report of the Intergovernmental Panel on Climate Change, IPCC, 2014.

758 Parkhurst, D. L., and Appelo, C.: User’s guide to PHREEQC (Version 2): A computer program for speciation, batch-reaction,  
759 one-dimensional transport, and inverse geochemical calculations, US Geological Survey, Denver, 326 pp., 1999.

760 Peters, S. C., Blum, J. D., Driscoll, C. T., and Likens, G. E.: Dissolution of wollastonite during the experimental manipulation  
761 of Hubbard Brook Watershed 1, *Biogeochemistry*, 67, 309–329, 10.1023/B:BIOG.0000015787.44175.3f, 2004.

762 Renforth, P.: The potential of enhanced weathering in the UK, *International Journal of Greenhouse Gas Control*, 10, 229–243,  
763 2012.

764 Rogelj, J., Shindell, D., Jiang, K., Fifita, S., Forster, P., Ginzburg, V., Handa, C., Kheshgi, H., Kobayashi, S., Kriegler, E.,  
765 Mundaca, L., Séférian, R., and Vilariño, M.: Mitigation Pathways Compatible with 1.5°C in the Context of Sustainable  
766 Development, 2018.

767 Rosi-Marshall, E. J., Bernhardt, E. S., Buso, D. C., Driscoll, C. T., and Likens, G. E.: Acid rain mitigation experiment shifts a  
768 forested watershed from a net sink to a net source of nitrogen, *Proceedings of the National Academy of Sciences*, 113, 7580–  
769 7583, 2016.

770 Schaberg, P. G., Miller, E. K., and Eagar, C.: Assessing the threat that anthropogenic calcium depletion poses to forest health  
771 and productivity, US Department of Agriculture, Forest Service, Pacific Northwest and Southern Research Stations, Portland,  
772 OR, 37–58, 2010.

773 Schlesinger, W. H., and Amundson, R.: Managing for soil carbon sequestration: Let’s get realistic, *Global Change Biology*,  
774 00, 1–4, 10.1111/gcb.14478, 2018.

775 Sebestyen, S. D., Boyer, E. W., and Shanley, J. B.: Responses of stream nitrate and DOC loadings to hydrological forcing and  
776 climate change in an upland forest of the northeastern United States, *Journal of Geophysical Research: Biogeosciences*, 114,  
777 G02002, 2009.

778 Shao, S., Driscoll, C. T., Johnson, C. E., Fahey, T. J., Battles, J. J., and Blum, J. D.: Long-term responses in soil solution and  
779 stream-water chemistry at Hubbard Brook after experimental addition of wollastonite, *Environ. Chem*, 13, 528–540, 2016.

780 Sims, R., Schaeffer, R., Creutzig, F., Cruz-Núñez, X., D’agosto, M., Dimitriu, D., Figueroa Meza, M., Fulton, L., Kobayashi,  
781 S., and Lah, O.: *Transport*, Cambridge University Press, Cambridge and New York, 2014.

782 Sopper, W. E., and Lull, H. W.: The representativeness of small forested experimental watersheds in northeastern United  
783 States, *International Association of Hydrological Sciences*, 66, 441–456, 1965.

784 Stamboliadis, E., Pantelaki, O., and Petrakis, E.: Surface area production during grinding, *Minerals engineering*, 22, 587–592,  
785 2009.

786 Strefler, J., Amann, T., Bauer, N., Krieglner, E., and Hartmann, J.: Potential and costs of carbon dioxide removal by enhanced  
787 weathering of rocks, *Environmental Research Letters*, 13, 034010, 2018.

788 Teien, H.-C., Kroglund, F., Åtland, Å., Rosseland, B. O., and Salbu, B.: Sodium silicate as alternative to liming-reduced  
789 aluminium toxicity for Atlantic salmon (*Salmo salar* L.) in unstable mixing zones, *Science of the total environment*, 358, 151-  
790 163, 2006.

791 Traaen, T., Frogner, T., Hindar, A., Kleiven, E., Lande, A., and Wright, R.: Whole-catchment liming at Tjønnsstrond, Norway:  
792 an 11-year record, *Water, Air, and Soil Pollution*, 94, 163-180, 1997.

793 Emissions & Generation Resource Integrated Database (eGRID): [https://www.epa.gov/sites/production/files/2018-  
794 02/eGRID2016\\_all\\_files\\_since\\_1996.zip](https://www.epa.gov/sites/production/files/2018-02/eGRID2016_all_files_since_1996.zip), access: 25 October, 1999.

795 Minerals Yearbook: Wollastonite: <https://www.usgs.gov/centers/nmic/wollastonite-statistics-and-information>, access: 11  
796 September 2000.

797 Zhao, Y., Duan, L., Xing, J., Larssen, T., Nielsen, C. P., and Hao, J.: Soil acidification in China: is controlling SO<sub>2</sub> emissions  
798 enough?, *Environmental Science & Technology*, 43, 8021–8026, 10.1021/es901430n, 2009.

799

800

801